Comparisons between the pendulum with varying length and the pendulum with oscillating support

James A. Wright[a], Michele Bartuccelli[a,*], Guido Gentile[b]

[a] *Department of Mathematics, University of Surrey, Guildford, GU2 7XH, UK*
[b] *Dipartimento di Matematica e Fisica, Università di Roma Tre, 00146 Roma, Italy*

Abstract

We consider two forced dissipative pendulum systems, the pendulum with vertically oscillating support and the pendulum with periodically varying length, with a view to draw comparisons between their behaviour. We study the two systems for values of the parameters for which the dynamics are non-chaotic. We focus our investigation on the persisting attractive periodic orbits and their basins of attraction, utilising both analytical and numerical techniques. Although in some respect the two systems have similar behaviour, we find that even within the perturbation regime they may exhibit different dynamics. In particular, for the same value of the amplitude of the forcing, the pendulum with varying length turns out to be perturbed to a greater extent. Furthermore the periodic attractors persist under larger values of the damping coefficient in the pendulum with varying length. Finally, unlike the pendulum with oscillating support, the pendulum with varying length cannot be stabilised around the upward position for any values of the parameters.

1. Introduction

Perturbations of the simple pendulum exhibit an extremely rich variety of dynamics whilst still allowing a complete control over the unperturbed system. For this reason perturbed pendula are often used as toy models to study new phenomena in dynamics — for instance in [3, 22, 50, 61, 60, 65] — or act as simplified models for more complex real world systems — see [47, 58, 63]. One of the most commonly studied perturbations is the pendulum with vertically oscillating support [6, 12, 13, 31, 65], often also referred to as the parametrically forced pendulum, see for example [22, 30, 33, 45, 67]. Another much studied perturbation of the simple pendulum is the pendulum with periodically varying length [8, 17, 59, 19, 57]. In [23, 54] it was noted that the pendulum with varying length is an example of a periodically forced system whose linearisation is different from Mathieu's equation, but no further analysis was completed. A brief comparison between the pendulum with oscillating support and the pendulum with varying length was made in [19], drawing the conclusions that the two systems are qualitatively different and further comparison of the two systems deserved a separate study. However there has not been further work focused on exploring the differences of the two systems. In fact, there are still instances, even as recent as 2014 [28], where the two systems are mistaken with one another — see also [36, 52, 53]. Therefore to avoid further confusion and misguidance it is important not only to highlight the differences between the two systems but also

*Corresponding author. Tel: +44(0)1483 682625 Fax: +44(0)1483 686071
Email addresses: `j.wright@surrey.ac.uk` (James A. Wright), `m.bartuccelli@surrey.ac.uk` (Michele Bartuccelli), `gentile@mat.uniroma3.it` (Guido Gentile)

Preprint submitted to Elsevier *January 9, 2017*

to note where they are similar to one another. In the present paper we expand on the study made in [19] and directly compare some aspects of the two systems.

The motion of a simple pendulum with length ℓ_0 is governed by the equation

$$\ddot{\theta}(s) + \frac{g}{\ell_0}\sin\theta(s) = 0, \tag{1}$$

where $\theta(s)$ is the angle between the pendulum and the downward vertical, g is the acceleration due to gravity and the dots denote derivatives with respect to the time s.

Consider a perturbation of the pendulum with fixed length ℓ_0 which is subject to frictional forces and whose pivot oscillates vertically with amplitude a and frequency ω. The non-dimensionalised equation of motion is

$$\ddot{\theta}(t) + \gamma\,\dot{\theta}(t) + (\alpha - \delta\cos t)\sin\theta(t) = 0, \tag{2}$$

where

$$\alpha := \frac{g}{\ell_0\omega^2}, \qquad \delta := \frac{a}{\ell_0}, \qquad t := \omega s,$$

the *damping coefficient* γ is non-negative and the dots now denote derivatives with respect to the rescaled time t. Consider also a pendulum with fixed pivot, but whose length periodically varies with time s as $\ell(s) = \ell_0 + \ell_1\cos\omega s$, with $\ell_1 < \ell_0$. The non-dimensionalised equation of motion is

$$\ddot{\theta}(t) + \left(-\frac{2\varepsilon\sin t}{1+\varepsilon\cos t} + \zeta\right)\dot{\theta}(t) + \frac{\alpha}{1+\varepsilon\cos t}\sin\theta(t) = 0, \tag{3}$$

where

$$\alpha := \frac{g}{\ell_0\omega^2}, \qquad \varepsilon := \frac{\ell_1}{\ell_0}, \qquad t := \omega s,$$

the *damping coefficient* ζ is non-negative and again the dots denote derivatives with respect to t.

It may be seen that the parameters α in the two equations (2) and (3) correspond to one another, as both the systems are perturbations of the simple pendulum (1). As a consequence, at least within the perturbation regime ($\delta, \varepsilon \ll 1$) it is not unreasonable to expect some similarities in the dynamics of the two systems with the same values of α. On the other hand, the *perturbation parameters* δ and ε appear very differently and in general there is no direct link between particular values of δ in the system (2) and ε in the system (3). Furthermore, as the perturbation parameters are increased, the two systems and their dynamics become increasingly different. We therefore focus our comparison of the two systems on the case δ, ε small, and show that even in this scenario they can exhibit significantly different dynamics.

In Section 2 we study the linearised equations of the two systems. In particular we study the *transition curves*, that is the curves in parameter space separating the regions of stable and unstable dynamics of the corresponding linearised systems. Here, a first difference between the two systems appears. Whilst it is well known [62, 41, 1, 2, 6, 13, 31] that for α sufficiently small and δ chosen accordingly, it is possible to stabilise the upward fixed point $(\theta, \dot{\theta}) = (\pi, 0)$ for the system (2), on the contrary, as already observed in [19], stability of the upward fixed point cannot be achieved for any values of the parameters in the system (3). From a physical perspective, one can argue that the excitation force caused by varying length is directed along the rod of the pendulum, and hence cannot create restoring torque to stabilise the upward position. Unstability of the upward position also follows from the computation of the first transition curve in Appendix A. In Section 3 we calculate sufficient conditions on the damping coefficient in each system for the origin to achieve global attraction (up to a zero measure set). In Section 4 we investigate analytically the subharmonic solutions, which represent the dominant attractors of the two systems in the perturbation regime. In particular we give results for the *threshold values*, that is the values of the damping coefficient under which such attractors persist. The threshold values from the first order calculations are compared with results from numerical simulations, from which we find that the system (2) is more suited to study by perturbation theory than the system (3), where higher order approximations may be necessary to achieve the same level of accuracy. In Section 5 we investigate the systems by means of numerical analysis and compare results concerning the phase curves of the attracting solutions as well as the sizes and topology of their corresponding basins of attraction. In Section 6 we study and compare the bifurcation structures of the two systems, which we relate to the results contained in the previous sections. In Section 7 we provide concluding remarks and comment on some open problems.

2. Linearised systems

We first consider the linearisation of the system (2) for which we wish to study the stability of the two fixed points. Linearising about the downward ($\theta = 0$) and upward ($\theta = \pi$) fixed points, respectively, results in the two equations

$$\ddot{\psi}(t) + (\alpha - \delta \cos t)\, \psi(t) + \gamma\, \dot{\psi}(t) = 0, \tag{4a}$$

$$\ddot{\psi}(t) - (\alpha - \delta \cos t)\, \psi(t) + \gamma\, \dot{\psi}(t) = 0, \tag{4b}$$

where ψ represents the angle between the pendulum and the downward and upward vertical, respectively. It is evident, due to the properties of $\cos t$, that a change in the sign of δ is equivalent to a shift of π in time t, hence the invariant curves do not depend on the sign of δ [12]. Therefore, even though changing the sign of α makes little sense physically (since α is proportional to positive constants by definition), for the purpose of both analytical computations and numerical simulations it is convenient to consider only the equation (4a) and change the sign of α when studying the stability of the upward position. Setting $\gamma = 0$, the linearisation of (2) about either one of its fixed points results in Mathieu's equation, a special case of Hill's equation, see [46, 5, 40].[1]

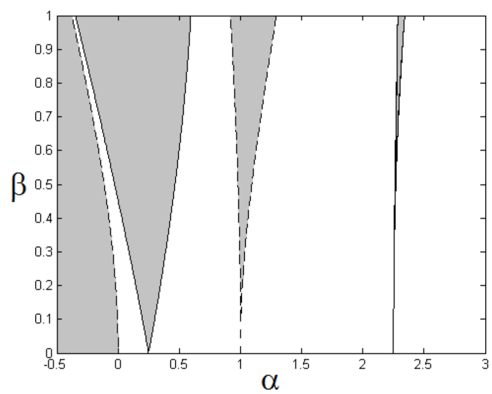

Figure 1: Transition curves for the linearised system of the pendulum with oscillating support (2) with $\gamma = 0$. The dashed lines correspond to 2π-periodic solutions and the solid lines to 4π-periodic solutions. The shaded regions are those in which the solutions are unstable (and hence are called instability tongues).

[1] Usually, in particular in mathematics textbooks, Mathieu's equation is written as $\ddot{\psi} + (\alpha + \delta \cos 2t)\psi = 0$; however we shall use the writing with $\cos t$, following [12, 40], more natural from a physical point of view.

By Floquets theorem [46, 40] the curves on which the period 2π and period 4π solutions occur separate the regions of parameter space where all solutions of (4a) are bounded from the regions where unbounded solutions may occur. Such curves, usually referred to as *transition curves*, can be computed by standard algorithms; see for instance [40, Chapter 9]. The regions of stability and instability are shown in Figure 1: choosing values of the parameters α and δ inside the white regions results in *stable solutions*, whilst for parameters chosen in the grey regions the solutions are *unstable*, according to Magnus and Winkler's terminology [46].

We now consider the pendulum with varying length. Instability domains in parameter space for the system with $\zeta > 0$ have been previously calculated in [17, 19, 59]. Here we wish to compute the transition curves when $\zeta = 0$, for comparison with those of the system (2). For $\zeta = 0$, in terms of the new variable $\Theta(t) := \ell(t)\theta(t)$, the system (3) may be put into a form[2] which does not contain any term involving $\dot{\theta}$:

$$\ddot{\Theta}(t) + \frac{\varepsilon\cos(t)}{1+\varepsilon\cos t}\Theta(t) + \alpha\ell_0 \sin\left(\frac{\Theta(t)}{\ell_0(1+\varepsilon\cos t)}\right) = 0. \tag{5}$$

Linearising (5) about the downward fixed point ($\theta = \Theta = 0$) we obtain an equation in the form of Hill's equation, given by

$$\ddot{\psi}(t) + \frac{\alpha+\varepsilon\cos t}{1+\varepsilon\cos t}\psi(t) = 0, \qquad \varepsilon < 1. \tag{6}$$

The above is not in the form of Mathieu's equation, as previously noted [23], however keeping only the terms at first order in ε yields

$$\ddot{\psi}(t) + \Big(\alpha + \varepsilon(1-\alpha)\cos t\Big)\psi(t) = 0, \tag{7}$$

which is of the form of Mathieu's equation, even though now the parameter α appears in the forcing term as well. By calculating the transition curves in the same way as previously for the pendulum with oscillating support, we find the regions of stability and instability for equation (7) as shown in Figure 2(a). There are three important points to note:

1. The transition curves appear different from the transition curves for Mathieu's equation (4a). This is a consequence of the forcing coefficient in (7) depending also on the parameter α. In particular the unstable tongue which emanates from $\alpha = 1$ has completely vanished. This was also noted in Section 3 of [19].
2. The first order approximation to (6) results in a system of the form of Mathieu's equation. Therefore it is not surprising that there exist stable regions for $\alpha < 0$. However this does not correspond to the stability of the upward fixed point for the pendulum with varying length. Indeed, when considering higher order approximations the transition curves change drastically. For instance, approximating the linearised system (6) as far as $\mathcal{O}(\varepsilon^8)$, we find the stability curves shown in Figure 2(b). For $\alpha > 0$ the curves show good agreement with those in Figure 2(a) only for $\varepsilon \ll 1$, whilst for $\alpha < 0$ the stable region has almost vanished: the first transition curve, that is the transition curve emanating from the origin, becomes more and more close to the vertical axis. To obtain the transition curves for the full linearised system (6) a careful analysis is needed, because the higher order corrections become more and more relevant when ε becomes close to 1. This has been done in [4], by using a combination of

[2]The transformation to Θ may also be written in the form $\Theta(t) = \ell(t)\theta(t) = e^{\frac{1}{2}\int a(t)\,\mathrm{d}t}\theta(t)$, with $a(t) := 2\dot{\ell}(t)/\ell(t)$, which is the standard transformation used to cast Hill's equation in Hamiltonian form [46, 15].

both analytical and numerical methods. In fact, in [4] only the region of positive α has been considered explicitly, however it is not difficult to show that the first transition curve is the axis $\alpha = 0$, see Appendix A.

3. More care must be taken when considering the stability of the upward position $\theta = \pi$. The transformation $\Theta = \ell\theta$ does not preserve both fixed points of the system (3): under that transformation $\theta = 0$ is mapped into $\Theta = 0$, while $\theta = \pi$ is mapped into $\Theta = \pi\ell_0(1 + \varepsilon\cos t)$, thus the hyperbolic fixed point $\theta = \pi$ corresponds to a hyperbolic orbit of order ε in the Θ coordinates. However, if we consider the original system (3) with $\zeta = 0$ and transform to the coordinates $\varphi = \theta - \pi$ we obtain the system

$$\ddot{\varphi}(t) - \frac{2\varepsilon\sin t}{1 + \varepsilon\cos t}\dot{\varphi}(t) - \frac{\alpha}{1 + \varepsilon\cos t}\sin\varphi(t) = 0,$$

which is the same as equation (3), except for a change in sign of α. Transforming to coordinates $\Phi(t) = \ell(t)\varphi(t)$ and linearising around $\Phi = 0$, we obtain a system of the form (6), where only the sign of α is changed. Therefore, by changing the sign of α in equation (6) we are still able to obtain the stability of the inverted position $\theta = \pi$. As remarked in the previous comment, there is no stability region in the half-plane $\alpha < 0$, so that we conclude that the upward position is always linearly unstable for the pendulum with varying length.

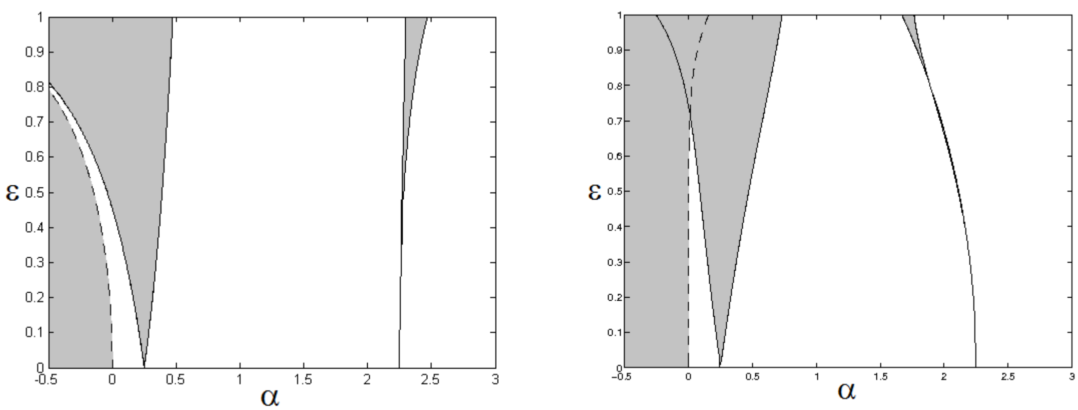

(a) (b)

Figure 2: Figure (a) shows the transition curves for the linearised system described by the equation (7). The dashed and solid lines correspond to the 2π-periodic and 4π-periodic solutions, respectively. The shaded regions are those in which the solutions are unstable. Figure (b) shows transition curves for an $\mathcal{O}(\varepsilon^8)$ approximation of equation (6). The transition curves for the full linearised system (6) can be found in [4].

As far as the full nonlinear systems are concerned, when the fixed points are linearly unstable we can conclude that *a fortiori* they are unstable as well. In particular the pendulum with varying length cannot be stabilised around its upward fixed point for any values of the parameters. To deduce stability from linear stability, that is for values of the parameters inside the stability regions of the linearised systems, requires a more delicate analysis, involving KAM-type arguments [6, 14].

3. Global attraction to the origin

We now return to the full nonlinear systems (2) and (3). To compute the conditions for which the origin attracts the full phase space, up to a zero-measure set, we use the approach outlined in [11]; see also [9, 65]. First we consider the system (2) and define $f(t)$ as

$$f(t) := \alpha - \delta \cos(t) \tag{8}$$

with the requirement $f(t) > 0$. The consequences of this restriction are that the method can only be applied to the pendulum centred about $\theta = 0$ and $|\delta| < \alpha$. By applying the Liouville transformation

$$\tau = \int_0^t \sqrt{f(u)}\,\mathrm{d}u \tag{9}$$

and introducing the variable $x(\tau) = \theta(t)$, we write the equation (2) in terms of the new time τ as a first order ODE on $\mathbb{T} \times \mathbb{R}$,

$$x' = y, \qquad y' = -\frac{y}{\sqrt{F}}\left(\frac{F'}{2\sqrt{F}} + \gamma\right) - \sin x, \tag{10}$$

where the dashes represent derivatives with respect to τ and $F(\tau) := f(t)$. By setting $E(x, y) := 1 - \cos x + y^2/2$ and $\mathcal{H}(\tau) := E(x(\tau), y(\tau))$, one finds $\mathcal{H}' \leq 0$ provided γ satisfies

$$\gamma > \gamma_0 := -\min_{\tau \geq 0} \frac{F'}{2\sqrt{F}} = -\min_{t \geq 0} \frac{\dot{f}}{2f} = -\min_{t \geq 0} \frac{\delta \sin t}{2(\alpha - \delta \cos t)}. \tag{11}$$

In [65, Appendix 1] it is proven that under the condition (11) all trajectories move towards the origin, up to a zero measure set of initial conditions, and hence the basin of attraction of the origin has full measure for $\alpha > 0$ and $|\delta| < \alpha$.

The conditions for global attraction to the origin for the pendulum with varying length are studied in a similar way. In this instance we define $h(t)$ and $g(t)$ as

$$h(t) := \frac{\alpha}{1 + \varepsilon \cos t}, \qquad g(t) := -\frac{2\varepsilon \sin t}{1 + \varepsilon \cos t}, \tag{12}$$

and again require $h(t) > 0$, which results in the restrictions $\alpha > 0$ and $\varepsilon < 1$. Applying the Liouville transformation (9), with h instead of f, and setting $x(\tau) = \theta(t)$, the system may be written in terms of the new time τ as

$$x' = y, \qquad y' = -\frac{y}{\sqrt{H}}\left(\frac{2G + H'}{2\sqrt{H}} + \zeta\right) - \sin x, \tag{13}$$

where again the dashes represent derivatives with respect to τ and $H(\tau) := h(t)$, $G(\tau) := g(t)$. There is a clear similarity between the equations (13) for the pendulum with varying length and (10) for the pendulum with oscillating support. The analysis follows through in exactly the same manner and it is found that the origin attracts a full measure set of phase space provided ζ satisfies

$$\zeta > \zeta_0 := -\min_{\tau \geq 0} \frac{2G + H'}{2\sqrt{H}} = -\min_{t \geq 0} \frac{2g\sqrt{h} + \dot{h}}{2h} = -\min_{t \geq 0}\left(\frac{\varepsilon \sin t}{2(1 + \varepsilon \cos t)} - \frac{2\varepsilon \sin t}{\sqrt{\alpha(1 + \varepsilon \cos t)}}\right). \tag{14}$$

For instance, for $\alpha = 0.5$ and $\varepsilon = \delta = 0.1$ one finds $\gamma_0 \approx 0.102$ and $\zeta_0 \approx 0.334$. The numerical computations reported in Section 5 show that in fact the origin attracts almost every trajectory even for smaller values of the damping coefficient: taking $\gamma > \gamma_1$ or $\zeta > \zeta_1$, with $\gamma_1 \approx 0.060$ and $\zeta_1 \approx 0.090$, turns out to be enough. As expected, condition (14) on ζ for the pendulum with varying length has some similarity to that in (11) for the pendulum with oscillating support. However for the system of the pendulum with varying length we find that damping coefficient must be taken larger, so as to exceed the forcing also created by the term $g(t)$. This shows that the periodic attractors of (3) are more robust and persist under larger values of the damping coefficient. This could be expected by looking at (3), since the coefficient of $\dot{\theta}(t)$ is not of definite sign for $\zeta = 0$.

4. Threshold values of the subharmonic solutions

A solution to (2) or (3) is said to be in a $p\!:\!q$ *resonance* with the forcing if it completes p cycles, before closing, every q periods of the forcing. According to standard terminology [56, 24], such a solution represents a *subharmonic solution* of order q. In this section we shall be interested in subharmonic solutions which depend on the perturbation parameter so as to reduce to periodic solutions of the unperturbed pendulum as the parameter goes to zero; thus, they will be refered to as *perturbative subharmonic solutions*. As we shall see in Section 5, subharmonic solutions which do not have such a property may appear as well: we shall call the latter *non-perturbative subharmonic solutions*.

The *threshold values* for the two systems are the largest values of γ or ζ under which a periodic solution which is in a $p\!:\!q$ resonance with the forcing persists. For δ or ε small, respectively, the periodic solutions which are perturbative subharmonic solutions exist for all values of the damping coefficient below the corresponding threshold. Moreover the threshold values may be calculated using perturbation techniques. The method is described, for instance, in [7], where it was used for a forced cubic oscillator, and has since been applied to the spin-orbit system [10] and the pendulum with oscillating support [65]. To implement the method, one writes γ and ζ as power series in δ and ε, respectively, as $\gamma = \delta B_1 + \delta^2 B_2 + \delta^3 B_3 + \dots$ and $\zeta = \varepsilon C_1 + \varepsilon^2 C_2 + \varepsilon^3 C_3 + \dots$ and computes the coefficients B_i, C_i at each level, by requiring that there is a periodic solution to all orders of perturbation theory. For any given resonance, there will be a first non-zero coefficient, say B_k for some $k \in \mathbb{N}$ for the system (2), such that $B_k \varepsilon^k$ provides an approximate value of the corresponding threshold value, while the higher order contributions only provide small corrections to these values.

For the pendulum with oscillating support, in [65, Section 2] we derived the equations of motion in terms of the action-angle variables and looked for the conditions for perturbative subharmonic solutions to exist. To zeroth order one finds the resonance conditions $\pi\sqrt{\alpha}/2\mathbf{K}(k_1) = p/q$ for oscillating solutions inside the separatrix and $\pi\sqrt{\alpha}/2k_2\mathbf{K}(k_2) = p/q$ for rotating solutions outside, with $p, q \in \mathbb{N}$ — we refer to [65] for notations (see also Appendix B below). This fixes the resonance $p\!:\!q$. To first order, in both cases, we need $p = 1$ and q to be even for B_1 not to vanish, see also [43]. The corresponding values of the coefficients $B_1 = B_1(p/q)$ for the system with $\alpha = 0.5$ are given in Tables 1 and 2; the values k_1 and k_2 are the elliptic moduli corresponding to each solution. It is

q	k_1	$B_1(1/q)$
2	0.885201568846	0.597944
4	0.998888384493	0.489649
6	0.999986981343	0.487616
8	0.999999846887	0.487578
10	0.999999998199	0.487577
12	0.999999999979	0.487577

Table 1: Constants B_1 for the oscillating attractors of the pendulum with oscillating support with $\alpha = 0.5$.

q	k_2	$B_1(1/q)$
2	0.924397052341	0.432005
4	0.998899257272	0.485542
6	0.999986983601	0.487439
8	0.999999846887	0.487577
10	0.999999998199	0.487577
12	0.999999999978	0.487577

Table 2: Constants B_1 for the rotating attractors of the pendulum with oscillating support with $\alpha = 0.5$.

q	k_1	$C_1(1/q)$
2	0.885201568846	0.896916
4	0.998888384493	0.734474
6	0.999986981343	0.731424
8	0.999999846887	0.731354
10	0.999999998199	0.731279
12	0.999999999979	0.731747

Table 3: Constants C_1 for the oscillating attractors of the pendulum with varying length with $\alpha = 0.5$.

q	k_2	$C_1(1/q)$
2	0.924397052341	0.648007
4	0.998899257272	0.728313
6	0.999986983601	0.731309
8	0.999999846887	0.731365
10	0.999999998199	0.731363
12	0.999999999978	0.729694

Table 4: Constants C_1 for the rotating attractors of the pendulum with varying length with $\alpha = 0.5$.

expected that the threshold values for attractors whose period is an odd multiple of the forcing are found at the second order in the power series, that is that B_2 does not vanish for $p = 1$ and $q \in \mathbb{N}$: thus, $\varepsilon^2 B_2$ provides a second order correction to εB_1 for q even, while it represents the dominant contribution for q odd. We refer once more to [65, Section 2] for details.

For the pendulum with varying length, one can reason in a similar way; details can be found in Appendix B. Of course the equations of the two systems coincide when $\delta = \varepsilon = 0$: this is a result of the two systems sharing the same unperturbed system. In particular the resonance condition is the same in both systems. To first order, we find again the conditions $p = 1$ and q even for C_1 not to vanish. The corresponding values of the coefficients $C_1 = C_1(p/q)$ for $\alpha = 0.5$ are given in Tables 3 and 4; the values k_1 and k_2 are the elliptic moduli corresponding to each solution.

For both systems with $\alpha = 0.5$, as q is increased, the values of $B_1(1/q)$ and $C_1(1/q)$ approach limit values: approximately 0.488 for the pendulum with oscillating support and 0.731 for the pendulum with varying length. Nevertheless, for a fixed value of δ or ε, only a finite number of attractors are found; this phenomenon was already observed in [65], and we refer to that paper for an explanation. In particular, by setting $\delta = \varepsilon = 0.1$, inside the separatrix for all values of γ and ζ below γ_1 and ζ_1, respectively, numerically we only find the attractor corresponding to the 1:2 resonance (OSC), besides the downward fixed point (FP). For the pendulum with oscillating support, the calculated value of $\delta B_1(1/2)$ is very close to the numerical result for the threshold value γ, see Table 5. On the contrary, for the pendulum with varying length, the calculated value of $\varepsilon C_1(1/2)$, as deduced from Table 3, does not match so closely to the numerical results for the threshold value ζ in Table 6.

	Basin of attraction %	
γ	FP	OSC
0.05970	98.59	1.41
0.05979	99.20	0.80
0.06000	100.00	0.00

Table 5: Relative areas of the basins of attraction for equation (2) with $\alpha = 0.5$ and $\delta = 0.1$

	Basin of attraction %	
ζ	FP	OSC
0.08900	94.94	5.06
0.09022	98.98	1.02
0.09023	100.00	0.00

Table 6: Relative areas of the basins of attraction for equation (3) with $\alpha = 0.5$ and $\varepsilon = 0.1$

	Basin of attraction %	
ζ	FP	OSC
0.0890	99.77	0.23
0.0896	99.95	0.05
0.0900	100.00	0.00

Table 7: Relative areas of the basins of attraction for equation (3) with $\alpha = 0.5$ and $\varepsilon = 0.01$

	Basin of attraction %	
ζ	FP	OSC
0.0890	96.13	3.87
0.0896	98.16	1.84
0.0900	100.00	0.00

Table 8: Relative areas of the basins of attraction for equation (15) with $\alpha = 0.5$ and $\varepsilon = 0.1$

In order to compute the threshold values at the first order in ε the functions $h(t)$ and $g(t)$ — see (12) — are approximated by $h_1(t) := \alpha(1 - \varepsilon \cos t)$ and $g_1(t) := -2\varepsilon \sin t$. Apparently the approximation to $h(t)$ is reasonable, however the approximation of $g(t)$ is significantly different. Taking ε smaller, we find the numerical results fit more closely with the computed threshold values, see Table 7 where $\varepsilon = 0.01$. Furthermore, if we replace $g(t)$ in (3) with $g_1(t)$, to obtain the system

$$\ddot{\theta}(t) + (-2\varepsilon \sin t + \gamma)\,\dot{\theta}(t) + \frac{\alpha}{1 + \varepsilon \cos t} \sin \theta(t) = 0, \tag{15}$$

the numerical results with $\varepsilon = 0.1$ better coincide with the first order calculations for the thresholds values — see Table 8. Therefore we can conclude that, for the chosen values of the parameters δ and ε, while the pendulum with oscillating support is well described by a first order perturbation analysis, in the case of the pendulum with varying length the higher order corrections are relevant and hence should be taken into account to match the numerical results.

5. Numerical results

We now consider the two pendulum systems (2) and (3), and estimate numerically the relative areas of the basins of attraction; previous study has be completed in [12, 65, 67] for the pendulum with oscillating support and in [17, 19] for the pendulum with varying length. Throughout all this section, we fix the parameter values at $\alpha = 0.5$ and $\delta = \varepsilon = 0.1$.

We take initial conditions from the same region $\mathcal{Q}$ of phase space used in [12, 65], namely $\theta \in [-\pi, \pi]$, $\dot{\theta} \in [-4, 4]$. This is due to the consideration that all the attracting solutions which are found are contained entirely inside the region $\mathcal{Q}$. By collecting together all points whose trajectories end up on the same attractor, we reconstruct the corresponding basins of attraction. The percentage of points belonging to the same basin of attraction provides an estimate of its relative area with respect the sample region $\mathcal{Q}$. The simulations to calculate the relative areas of the basins of attraction used 300 000 pseudo-random initial conditions in $\mathcal{Q}$: with a 95% confidence interval [51], this corresponds to an approximation correct to the first or second decimal — see Table 1 in [66]

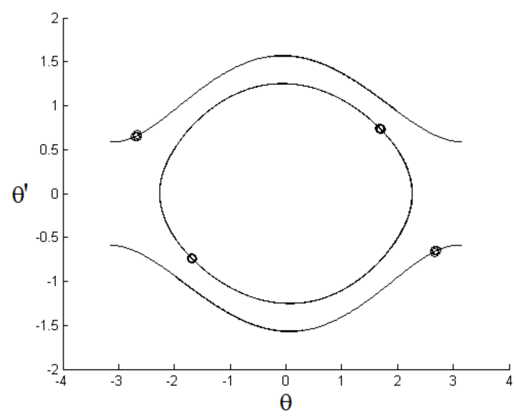

Figure 3: Attracting periodic solutions for the system (2) with $\alpha = 0.5$, $\delta = 0.1$ and $\gamma = 0.02$, namely two period-1 rotations (PR and NR) and one period-2 solution which oscillates about the downward fixed point (OSC). Periods can be deduced by circles corresponding to the Poincaré map.

For the chosen values of α and δ and for $\gamma \in [0.002, 0.06]$, the pendulum with oscillating support exhibits a set of four main attracting solutions, the fixed point $(\theta, \dot{\theta}) = (0, 0)$ (FP) and three subharmonic solutions: a positive rotating solution (PR), a negative rotating solution (NR) and an oscillating solution (OSC). For brevity, in the following, we shall say that a solution has period n if it comes back to its initial value after n times the forcing period. Under this convention, both the rotating solutions PR and NR (corresponding to 1:1 resonances) have period 1 and the oscillating solution OSC (corresponding to a 1:2 resonance) has period 2. Examples of the three periodic attractors are shown in Figure 3. In Table 9 and Figure 4 we give the corresponding relative areas of the basins of attraction for γ in the range investigated. A similar table and figure are shown in [65], where fewer values of γ were investigated. For $\gamma = 0.027$ we also find a fifth attractive solution,[3] which persists only in a small range of values for γ. Indeed it does not exist for $\gamma = 0.025$ or 0.030. The solution is an oscillation which is in a 5:10 resonance with the forcing, and attracts approximately 1.1% of phase space. Contrary to the main periodic attractors, it is a non-perturbative subharmonic solution, as it does not continue any periodic solution of the unperturbed system. Subharmonic solutions corresponding to resonances $p{:}q$, with p and q not relatively prime, were also found in [32], where it was remarked that they are stable over narrow parameter regions.

	Basin of attraction %		
γ	FP	PR/NR	OSC
0.00200	84.57	3.35	8.73
0.00500	79.91	3.88	12.32
0.01000	72.24	4.60	18.57
0.02000	71.95	4.57	18.90
0.02300	70.73	5.18	18.90
0.02500	69.28	5.19	20.35
0.03000	69.94	4.42	21.23
0.03300	68.92	3.75	23.59
0.03500	68.77	3.16	24.90
0.03700	70.76	2.51	24.23
0.04000	73.84	1.42	23.32
0.04300	78.12	0.15	21.59
0.04500	80.87	0.00	19.13
0.04700	82.88	0.00	17.12
0.05000	85.61	0.00	14.39
0.05300	87.95	0.00	12.05
0.05500	91.13	0.00	8.87
0.05900	96.96	0.00	3.04
0.05970	98.59	0.00	1.41
0.05979	99.20	0.00	0.80
0.06000	100.00	0.00	0.00

Table 9: Relative areas of the basins of attraction for the system (2) with $\alpha = 0.5$, $\delta = 0.1$ and different values of γ.

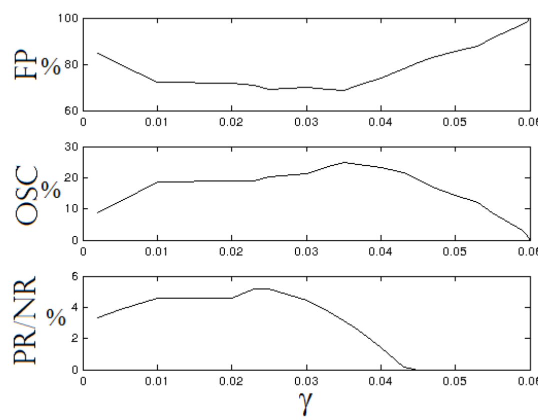

Figure 4: Plot of the relative areas of the basins of attraction for the system (2) with $\alpha = 0.5$, $\delta = 0.1$, for different values of γ as per Table 9.

For the same parameter values $\alpha = 0.5$ and $\varepsilon = 0.1$, the pendulum with varying length offers a wider variety of dynamics. As the calculations in Sections 3 and 4 show, the periodic attractors persist for larger values of the damping coefficient. As previously mentioned, even though both systems are perturbations of the same simple pendulum with $\alpha = 0.5$, there is not necessarily any

[3]This solution was not observed in [65], as the value $\gamma = 0.027$ was not studied there.

relation between the values of δ and ε. We have already seen that, by taking $\delta = \varepsilon$, the first order approximations for the threshold values are less accurate for the system (3) than for the system (2); this suggests that for a given value of the perturbation parameter the system (3) is further away from the unperturbed one. Indeed, even though the four main attractors of (3) are of the same kind as for the system (2) — that is FP, PR/NR and OSC —, in addition to these we also find six other non-perturbative subharmonic solutions. In particular, a second set of positive and negative rotations with period-1 (PR1/NR1), corresponding to 2:1 resonances, a set of positive and negative rotations with period 3 (PR3/NR3), corresponding to 3:3 resonances, and two oscillating attractors with period 4 (OSCL/OSCR) which are reflections of each other through the origin $(\theta, \dot{\theta}) = (0, 0)$, corresponding to 2:4 resonances. Examples of the persisting attractive solutions are shown in Figure 5 and the sizes of their corresponding basins of attraction are given in Tables 10 to 13.

The numerical results in Table 10 show that the solutions PR, NR and OSC persist for larger values of the damping coefficient in the system (3) than for the system (2): this is consistent with the calculations in Sections 3 and 4. Further to this, we also find that the periodic attractors PR3, NR3, OSCL and OSCR exist only in small windows of values for ζ. This is similar to the oscillation found for the pendulum with oscillating support for $\gamma = 0.027$. However for the pendulum with varying length, not only do we find four such attractors, but they exist for larger values of the damping

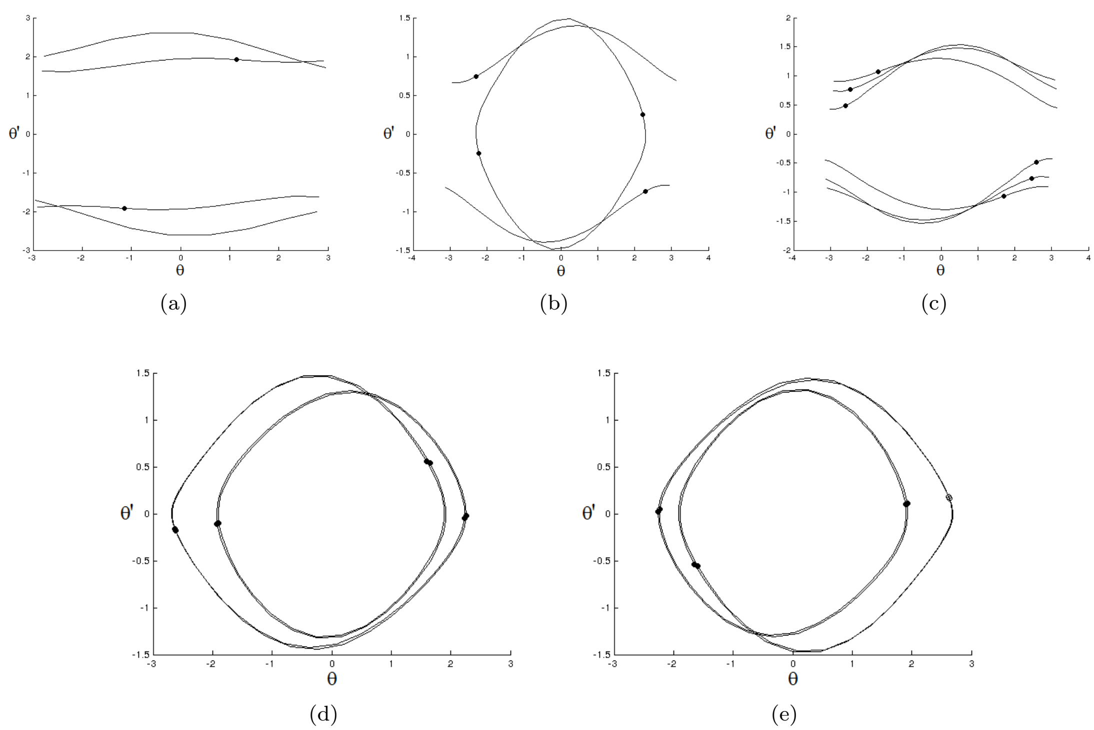

Figure 5: Examples of the attracting periodic solutions for the system (3) with $\alpha = 0.5$ $\varepsilon = 0.1$. Figure (a) shows the period-1 rotations PR1 and NR1 for $\zeta = 0.005$. Figure (b) shows the positive and negative rotations PR and NR and the period-2 oscillation OSC for $\zeta = 0.047$. Figure (c) shows the period 3 rotations PR3 and NR3 with $\zeta = 0.04$. Figures (d) and (e) show the period 4 oscillating solutions OSCL and OSCR, respectively, for $\zeta = 0.05$. The periods may be deduced from the circles corresponding to the Poincaré map.

	Basin of attraction %		
ζ	FP	PR/NR	OSC
0.00700	91.50	1.67	5.16
0.00900	90.98	1.77	5.48
0.01000	90.67	1.81	5.70
0.02000	83.39	2.90	10.81
0.03000	79.90	1.60	16.91
0.03700	78.28	1.59	18.53
$\vdots$	See Table 12		
0.04500	75.65	3.69	16.97
0.04700	73.86	3.82	18.50
0.04800	72.76	3.65	19.95
$\vdots$	See Table 13		
0.05500	73.00	2.94	21.12
0.06000	70.84	1.93	25.31
0.06500	73.39	0.26	26.10
0.06600	74.15	0.00	25.85
0.06700	74.29	0.00	25.71
0.07000	75.99	0.00	24.01
0.08000	84.83	0.00	15.18
0.08700	91.71	0.00	8.29
0.08800	93.14	0.00	6.86
0.08900	94.94	0.00	5.06
0.09000	97.62	0.00	2.38
0.09010	98.06	0.00	1.94
0.09020	98.71	0.00	1.29
0.09022	98.98	0.00	1.02
0.09023	100.00	0.00	0.00
0.09030	100.00	0.00	0.00

Table 10: Relative areas of the basins of attraction for the system (3) with $\alpha = 0.5$, $\varepsilon = 0.1$. The solutions are named as per Figure 5.

	Basin of attraction %			
ζ	FP	PR/NR	PR1/NR1	OSC
0.005	91.62	1.49	0.50	4.42
0.006	91.74	1.62	0.00	5.02

Table 11: Relative areas of the basins of attraction for the system (3) with $\alpha = 0.5$, $\varepsilon = 0.1$ and $\zeta = 0.005, 0.006$. The solutions are named as per Figure 5.

	Basin of attraction %			
ζ	FP	PR/NR	PR3/NR3	OSC
0.038	78.29	1.77	0.00	18.17
0.039	77.24	2.29	1.20	15.77
0.040	77.16	1.36	2.12	15.88
0.041	77.34	1.56	1.76	16.00
0.042	77.35	2.61	0.78	15.87
0.043	77.11	3.36	0.00	16.17

Table 12: Relative areas of the basins of attraction with $\alpha = 0.5$, $\varepsilon = 0.1$ and $\zeta \in [0.038, 0.043]$. The solutions are named as per Figure 5.

	Basin of attraction %			
ζ	FP	PR/NR	OSC	OSCL/R
0.049	71.58	3.53	21.36	0.00
0.050	71.30	3.67	17.79	1.79
0.051	71.21	3.68	18.09	1.67
0.052	71.52	3.54	21.40	0.00

Table 13: Relative areas of the basins of attraction with $\alpha = 0.5$, $\varepsilon = 0.1$ and $\zeta \in [0.049, 0.052]$. The solutions are named as per Figure 5.

coefficient. This gives further confirmation that the system is perturbed to a greater extent.

Upon comparing the curves in Figures 3 and 5(b) another difference between the two systems becomes clear. The oscillating attractors for the system (3) clearly cross the rotating attractors when projected into the phase plane — a behaviour not observed for the system (2). Through conservation of momentum, when the pendulum extends (or retracts) the angular velocity $\dot{\theta}$ decreases (or increases). Thus an oscillating solution may temporarily move faster than a rotating solution, without escaping the potential well. Another interesting difference is given by the rotations PR1/NR1 shown in Figure 5(a). Following the convention in [32] the rotating attractors corresponding to $r:n$ resonances, which complete r rotations in n periods of the forcing, are called (r, n) *orbits*. Then the rotations PR1/NR1 are classified as $(2, 1)$ orbits. In [32] the authors studied the system (2) and noted that, excluding transient behaviour, orbits with $r > n$ do not seem to appear. We find that such solutions do exist in the system (3) and attract a non-zero measure set of phase space for some values of the parameters. It may be that such solutions are also possible in the system (2), but, if so, they only occur for values of the parameters outside of those investigated here and in [32].

However, comparing Figures 4 and 6 it is also apparent that the basins of attraction for the two systems share some common traits. For both systems, when the damping coefficient is large enough, the downward fixed point attracts a full measure set of phase space. Decreasing the coefficient, the periodic attractors (PR/NR and OSC) appear and attract more of the phase space as γ and ζ continue to decrease. First the size of the basin of attraction of the period-2 oscillating attractor peaks and then begins to decrease as the size of the basins of attraction of the period-1 rotating attractors increases. Decreasing γ and ζ further, the periodic attractors attract less of the phase space and the basin of attraction belonging to the downward fixed point increases again. This was not observed for the cubic oscillator in [10], where decreasing the damping coefficient causes the basin of attraction of the fixed point to decrease. This is linked to the bifurcation structure of the two systems and the choice of parameters α, δ and ε. We shall return to this phenomenon in Section 6.

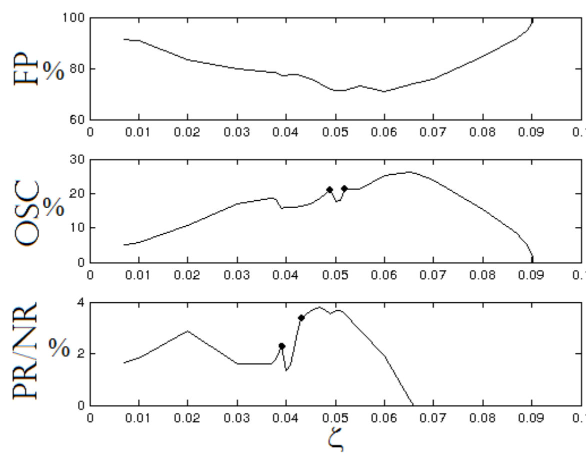

Figure 6: Relative areas of basins of attraction with $\alpha = 0.5$, $\varepsilon = 0.1$ and different values of ζ as per Tables 10, 12 and 13. The plots are labelled as in Table 10. Regions in which a solution is created or destroyed are marked with a dot. The basins of attraction for the solutions PR3/NR3 and OSCL/OSCR have not been included due to their small sizes and the low range of ζ under which the solutions persist.

Although the plots of the relative areas of the basins of attraction show similarities in their shape, for any particular value of the damping coefficient they are significantly different. For example, for $\gamma = 0.06$ the fixed point attracts a full measure set of phase space for the system (2), whilst in the system (3) with $\zeta = 0.06$ the period-1 rotations still persist and the period-2 oscillations attract approximately a quarter of phase space. In this sense, the basins of attraction for the two systems differ greatly, which is not surprising following the analysis of the previous sections. In Figure 7 we show the basins of attraction for $\gamma = \zeta = 0.02$ and 0.04. It is clear that not only do the sizes of the basins of attraction of similar attractors differ, but the regions of phase space attracted to given attractors also differ.

In Section 4, it was shown that the threshold values for the period-2 oscillations of the system (3) to first order is given by $\zeta \approx 0.8969\varepsilon$. Choosing $\varepsilon = 0.0667$ we have $\zeta = 0.8969\varepsilon \approx 0.0598$. This value matches with the threshold value of γ for the pendulum with oscillating support when $\delta = 0.1$. In Table 14 and Figure 8, we give the sizes of the basins of attraction for the system (3) with $\varepsilon = 0.0667$. Note that for $\zeta = 0.025$ we also find positive and negative rotations with 4:4 resonance, which each attract 0.57% of phase space. When the 4:4 rotations appear, the size of the fixed points basin of attraction reduces in size. When the 4:4 rotations disappear their basin of attraction is absorbed essentially by the 1:1 rotations; resulting in the increase in size shown in Table 14 for $\zeta = 0.027$. It is evident that both the sizes of the basins of attraction and the values at which attractors disappear are similar to the pendulum with oscillating support with $\delta = 0.1$, see Table 9.

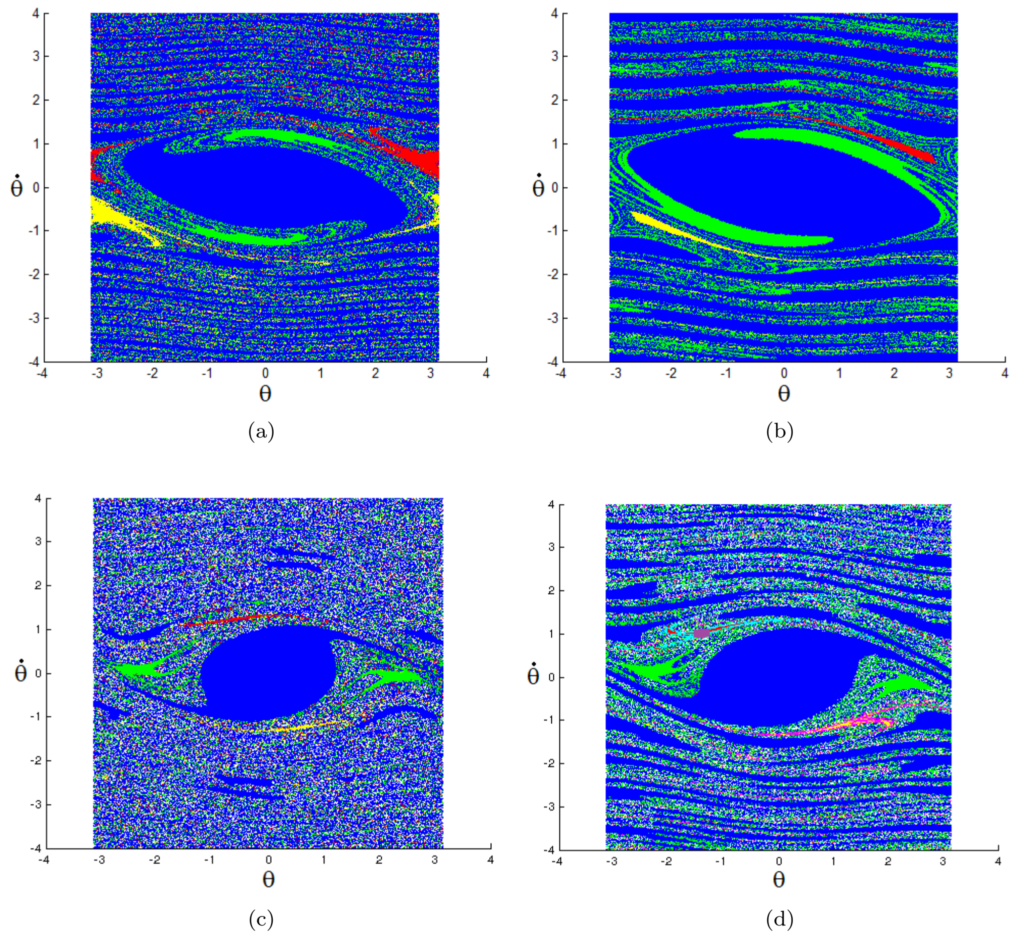

Figure 7: Basins of attraction for the two systems (2) and (3). The basins of attraction on the top correspond to the system (2) and those on the bottom to the system (3). Figures (a) and (c) show the basins of attraction for $\gamma = \zeta = 0.02$ and Figures (b) and (d) for $\gamma = \zeta = 0.04$. The basins are colour coded with the fixed points (FP) shown in blue, the period-2 oscillations (OSC) in green, the period-1 positive and negative rotating solutions (PR/NR) in red and yellow, respectively, and the period 3 positive and negative rotating solutions (PR3/NR3) in (d), for the pendulum with varying length, in cyan and magenta, respectively.

6. Bifurcation structures and regions of existence

The bifurcations in the pendulum with oscillating support have been extensively studied in the literature — see for instance [20, 21, 27, 30, 32, 33, 37, 39]. Usually, the location of the *bifurcation* *curves*, that is the curves in parameter space along which bifurcations occur, are investigated in terms of the amplitude and frequency of the forcing (more precisely in the ω-p plane for the equation $\ddot{\theta}(s) + \beta\omega\dot{\theta}(s) + (1 + p\cos\omega s)\,\sin\theta(s) = 0$), with the damping coefficient being fixed at a constant value. Here, first of all we shall describe the bifurcation curves for the system (2) in the α-δ plane, at constant γ: this frames the results of the quoted papers in the context of the parameters we use throughout.[4] The location of the curves will then be related to the damping coefficient γ and the results in Table 9. Finally we shall be able to explain the seemingly strange phenomenon, observed in [65], that the basin of attraction of the downward fixed point increases as γ decreases below 0.35 (as shown in Figure 4).

	Basin of attraction %		
ζ	FP	PR/NR	OSC
0.00500	79.53	4.44	11.60
0.01000	72.02	5.94	16.11
0.01500	70.55	3.93	21.59
0.02000	72.33	3.68	20.32
0.02500	68.48	3.90	22.61
0.02700	68.78	4.45	22.32
0.03000	68.40	4.25	23.11
0.03500	68.20	3.13	25.54
0.04000	73.40	1.39	23.82
0.04300	77.50	0.24	22.01
0.04500	80.39	0.00	19.61
0.05000	85.42	0.00	14.58
0.05500	91.27	0.00	8.73
0.05900	96.78	0.00	3.22
0.05970	98.34	0.00	1.67
0.05979	98.64	0.00	1.36
0.06000	100.00	0.00	0.00

Table 14: Relative areas of the basins of attraction for the system (3) with $\alpha = 0.5$, $\varepsilon = 0.0667$. The solutions are named as per Table 10.

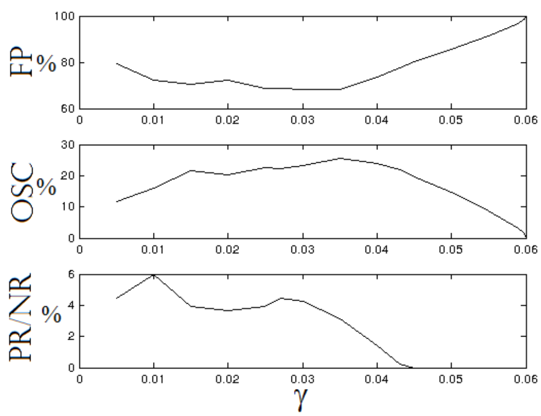

Figure 8: Plot of the relative areas of the basins of attraction for the system (3) with $\alpha = 0.5$, $\varepsilon = 0.1$, for different values of ζ as per Table 14.

Bifurcations in a dynamical system may be studied numerically by starting on a particular attractor and allowing a parameter of the system to slowly vary until the attractor either vanishes or bifurcates into another attractor. The bifurcation curves for the rotating attractors PR/NR with $\gamma = 0.05$ are shown in Figure 9(a). For fixed α, by increasing δ from zero the rotations appear by a saddle-node bifurcation at the curve A. For α large enough, by increasing δ further the rotations undergo a series of period doubling (also called flip) bifurcations, ultimately leading to chaos. The first and second period doubling bifurcations are marked in Figure 9(a) by the curves B and C, respectively. The curve above curve C marks the birth of a rotating chaotic attractor, which persists only in a very small interval of parameter values and disappears by a catastrophic bifurcation [20, 31, 33]. The appearance of chaotic attractors for small sets of parameter values and with small basins of attraction has been observed in similar contexts of multistable dissipative

[4]Due to the use of different parameters (more precisely to the fact that α is proportional to ω^{-2}), the images appear reversed when compared with those papers.

systems close to the conservative limit [35].

The bifurcation curves of the oscillating solution OSC are shown in Figure 9(b). Here the focus is on the region of parameter space around the primary instability tongue in Mathieu's equation (the curve marked as F in the figure). At the curve F the origin loses stability by a pitchfork bifurcation, which is supercritical to the left and subcritical to the right of the "turning point" c [21]. Indeed, if we fix α and let δ increase, to the left of c the stable fixed point bifurcates into a stable symmetric period-2 oscillation at the curve F, while to the right of c, along the curve D, a stable period-2 oscillation appears by a saddle-node bifurcation, together with an unstable period-2 oscillation which coalesces with the stable fixed point at the curve F. The curve E is where a symmetry breaking bifurcation takes place. Here the stable symmetric period-2 oscillation bifurcates into two stable asymmetric period-2 oscillations, which are reflections of each other through the origin [37]. At the curve G the asymmetric oscillations undergo a period doubling bifurcation. This is closely followed by a period doubling cascade which leads to chaos; which again persists only in a small interval of parameter values.

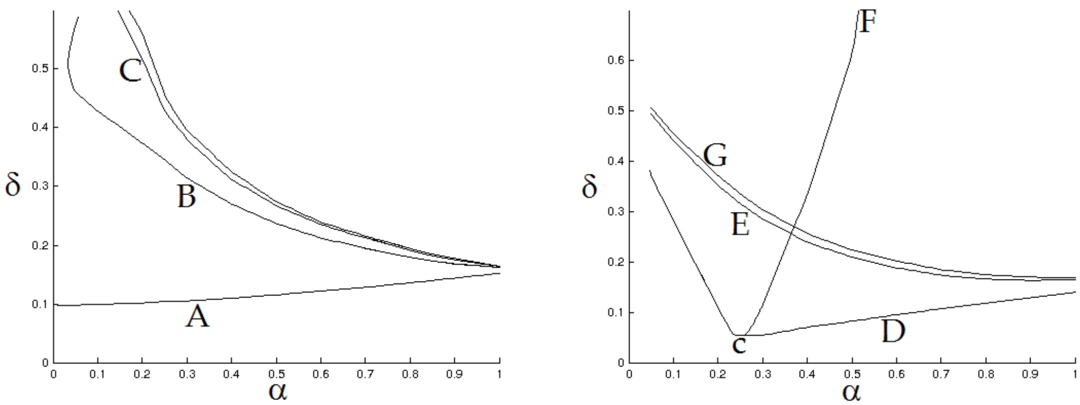

(a) (b)

Figure 9: Bifurcation curves for the equation (2) with fixed $\gamma = 0.05$. Figure (a) shows the bifurcation curves of the rotations PR/NR and (b) the curves of the oscillation OSC. For details see the text.

Note that the curve D can be obtained analytically from the perturbation theory calculations in Section 4, which allow one to express the threshold value for γ in terms of δ, for given α. In practice, for any fixed value of γ, we can invert the expression to deduce the value of δ at which the bifurcation occurs in terms of α. In that way, we construct the curve D in α-δ. It is evident that for $p = 1$, $q = 2$ and $\alpha < 1/4$ the resonance condition $\pi\sqrt{\alpha}q = 2\mathbf{K}(k_1)p$ can no longer be satisfied for $k_1 \in (0, 1)$, since $\mathbf{K}(k_1) > \pi/2$ for $k_1 > 0$ [44]. This agrees with the fact that the curve D terminates at $\alpha = 1/4$, that is in correspondence of the point c.

It is possible to stabilise the upward fixed point (that is to have stable oscillations about the upward vertical position $\theta = \pi$). However, as such solutions appear outside the perturbation regime, they are not comparable with the pendulum with varying length. Therefore, so as not to overwhelm Figure 9(b), the regions in which these solutions exist have not been included.

Increasing (decreasing) the value of damping coefficient γ causes the bifurcation curves for the rotating solutions shown in Figure 9(a) to move up and to the right (down and to the left). Similarly, by increasing (decreasing) the value of γ, the curves in Figure 9(b) move up (down). Hence a point corresponding to fixed values of α and δ in the system (2) may be found inside a given region of existence rather than another depending on the value of γ.

In particular, the point P corresponding to the values $\alpha = 0.5$, $\delta = 0.1$ is in a region of parameter space for which the fixed point is stable even when $\gamma = 0$, see Figure 1. Hence the fixed point remains asymptotically stable however small γ may be, as far as it is positive. As $\gamma \to 0$ the bifurcation curves move downward: the point c gets closer and closer to the α-axis and the point P turns out to be situated close to the curves B and E in Figure 9(a) and (b), respectively. By moving toward the edge of the region of existence of an attractor, the size of the corresponding basin of attraction decreases. As there are no new attractors in this region of parameter space, the basin of attraction of the fixed point increases, in agreement with Figure 4. Hence the increase is related to the location of parameters α and δ in respect to the regions of existence of the attractors at fixed γ, shown in Figure 9. In particular, by choosing (α, δ) either to the left of c in Figure 9(b) or in a region where the fixed point is unstable for $\gamma = 0$, this phenomenon would not be observed.

An analogous study of the bifurcation structure for the pendulum system (3) is not currently available elsewhere in the literature — see however [18, 19], where the bifurcation curves are derived for both rotations [19, Figure 1] and oscillations [19, Figure 2] and then compared with numerical results. The bifurcation curves for both the rotations PR/NR and oscillations OSC of the system (3) are shown in Figure 10(a) and (b), respectively. The curves are labeled so as to match with those in Figure 9.

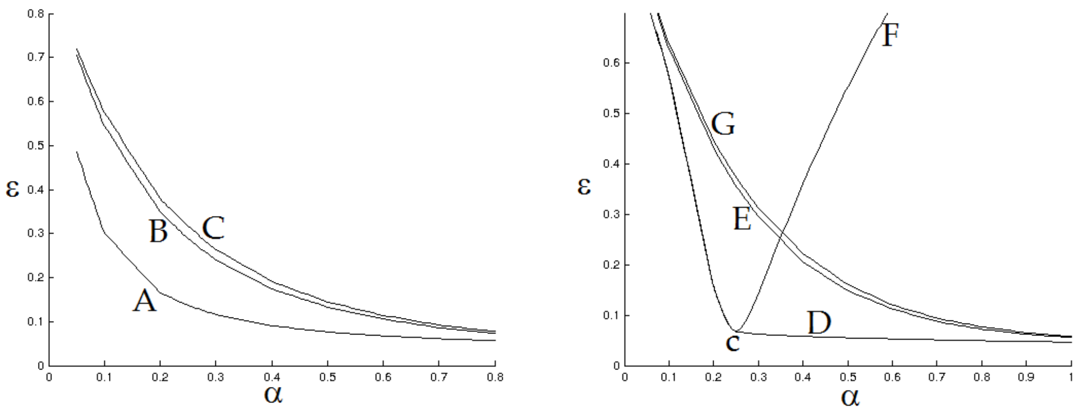

(a) (b)

Figure 10: Bifurcation curves for the system (3) with fixed $\zeta = 0.05$. Figure (a) shows the bifurcations curves of the rotations PR/NR and (b) the curves of the oscillation OSC. For details see the text.

Figure 10(a) shows the bifurcation structure of the rotating attractors PR/NR with $\zeta = 0.05$. The scenario is similar to that of the pendulum with oscillating support. At the curve A the rotating solutions appear at a saddle-node bifurcation. At the curve B the rotations undergo a period doubling bifurcation, resulting in 2:2 rotations. This is closely followed by a period doubling cascade starting at the curve C, which leads to chaos.

Figure 10(b) shows the bifurcation curves for the oscillation OSC with $\zeta = 0.05$. At D the oscillation becomes stable at a saddle-node bifurcation. At E the oscillation undergoes symmetry breaking, resulting in two asymmetric oscillations, still corresponding to 1:2 resonance. These asymmetric oscillations undergo a period doubling cascade starting at the curve G, which leads to chaotic dynamics. Note that the asymmetric oscillations created by the symmetry breaking bifurcation at E are different from the attractors OSCL and OSCR shown in Figure 5 (d) and (e), respectively.

Not only do the attractors OSCL and OSCR correspond to 2:4 resonance, but they also coexist with the oscillations OSC (corresponding to 1:2 resonances). At F the fixed point loses stability. The bifurcations which occur at the curve F are the same as in the pendulum with oscillating support (see previous discussion).

The bifurcation curves for the rotations in 2:1 and 3:3 resonances have not been included here, the reason being that they were not found for the pendulum with oscillating support and hence we are unable to make any comparison. However we found that the structure is analogous to that of the 1:1 rotations, but happens over a much smaller region of parameter space. In particular, by increasing ε the rotations PR1/NR1 and PR3/NR3 appear by a saddle-node bifurcation. By continuing to increase ε the attractors vanish. In the case of the 3:3 rotations this happens by a period doubling cascade, leading to chaos. The oscillations in a 2:4 resonance also appear by a saddle-node bifurcation as ε is increased. By increasing ε further, the asymmetric oscillations undergo a period doubling cascade, leading to chaotic dynamics; which again persist only in a small window of parameter values.

In the region of parameter space which surrounds the first tongue of instability for the corresponding linearised equation, see Figure 2, the bifurcations of the main attractors for the pendulum with varying length are the same as those for the corresponding attractors of the pendulum with oscillating support. However, if we were to consider the region around $\alpha = 1$ the structure would be quite different, owing to the lack of the unstable tongue in the corresponding linearised equation of the pendulum with varying length.

7. Conclusions

In the previous sections we contrasted two perturbations of the simple pendulum. It is found that the pendulum with varying length exhibits a wider variety of attractive solutions for the parameter $\alpha = 0.5$ and the same values for the forcing amplitudes $\delta = \varepsilon = 0.1$. The periodic attractors in the system (3) persist under larger values of the damping coefficient, a consequence of the extra forcing which naturally occurs in the coefficient of $\dot{\theta}$: this was observed numerically as well as in the threshold calculations of Section 4. By comparing Figures 9 and 10 in Section 6, we see that for $\alpha = 0.5$ and $\zeta = 0.05$ the regions of existence of the attractors are lower on the ε axis for the system (3), than they are on the δ axis for the system (2) with $\gamma = \zeta = 0.05$. However, for small α the opposite is true, the underlying reason behind this is unclear and deserves separate investigation.

It is evident from the analysis in Section 4 that the pendulum with varying length is well suited to study by perturbation theory only for smaller values of the perturbation parameter. This may be summed up by saying that the pendulum with varying length moves away from the unperturbed system more quickly as the perturbation parameter is increased. Furthermore, at the end of Section 5 we found that for $\varepsilon = 0.0667$ the pendulum with varying length exhibits similar dynamics to the pendulum with oscillating support with $\delta = 0.1$.

The numerical results show the two systems to be different both quantitatively and qualitatively. For example, for the parameter values investigated, apart from the main attractors, we found six extra attractors in the system of the pendulum with varying length: four rotating solutions and two oscillating solutions, compared with only one extra oscillating solution for the pendulum with oscillating support. However there are some similarities between the two systems which are apparent. The relative areas of the basins of attraction corresponding to the fixed points in both systems follow a similar curve, as do the period-1 rotations and period-2 oscillations; compare Figure 4 with Figure 6. The shape of these curves is different from those the cubic oscillator, see [10], where decreasing the damping coefficient leads to a decrease in the fixed points basin of attraction. The reason behind the increase in the size of the basin of attraction associated with the fixed point is related to the choice of parameters and the bifurcation structure of the two systems. The bifurcations which occur for the main, subharmonic attractors were also found to be the same. This is not surprising as the two systems share the same unperturbed system. However it is possible to choose α such that the bifurcation curves and the curves in Figures 4 and 6 appear quite different. For example, this may be achieved by taking $\alpha = 1$ and $\delta = \varepsilon$, so that the parameters lie inside the unstable region shown in Figure 1, which does not appear in Figure 2.

Acknowledgements This research was completed during the course of an EPSRC funded PhD.

Appendix A. Upside-down pendulum with varying length

The transition curves for Hill's equations, such as (6), are obtained by fixing $\alpha = \alpha(\varepsilon)$ in such a way that the corresponding solutions $\psi(t) = \psi(t, \varepsilon)$ are periodic with periods either 2π or 4π [46, 5, 40]. For ε small enough we look for solutions which depend analytically on ε. Therefore we write [40]

$$\alpha(\varepsilon) = \sum_{k=0}^{\infty} \varepsilon^k \alpha_k, \qquad \psi(t, \varepsilon) = \sum_{k=0}^{\infty} \varepsilon^k \psi_k(t), \tag{A.1}$$

and fix recursively the constants α_k in such a way that the functions $\psi_k(t)$ have all the same period 2π or 4π. By inserting (A.1) into (6) we obtain a sequence of equations,

$$\ddot{\psi}_0(t) + \alpha_0 \psi_0(t) = 0, \tag{A.2a}$$

$$\ddot{\psi}_k(t) + \sum_{\substack{k_1, k_2, k_3 \geq 0 \\ k_1 + k_2 + k_3 = k}} \alpha_{k_1} (-\cos t)^{k_2} \psi_{k_3}(t) + \cos t \sum_{\substack{k_1, k_2 \geq 0 \\ k_1 + k_2 = k-1}} (-\cos t)^{k_1} \psi_{k_2}(t) = 0, \qquad k \geq 1. \tag{A.2b}$$

For instance, to first orders, one has

$$\ddot{\psi}_1(t) + \alpha_0 \psi_1(t) - \alpha_0 \cos t \, \psi_0(t) + \alpha_1 \psi_0(t) + \cos t \, \psi_0(t) = 0, \tag{A.3a}$$

$$\begin{aligned} \ddot{\psi}_2(t) &+ \alpha_0 \psi_2(t) + \alpha_0 \cos^2 t \, \psi_0(t) + \alpha_2 \psi_0(t) - \alpha_0 \cos t \, \psi_1(t) \\ &+ \alpha_1 \psi_1(t) - \alpha_1 \cos t \, \psi_0(t) - \cos^2 t \, \psi_0(t) + \cos t \, \psi_1(t) = 0, \end{aligned} \tag{A.3b}$$

and so on. For $k = 0$ one must require $\alpha_0 = n^2/4$, with $n = 0, 1, 2, \ldots$, for the solution to be periodic with period 2π or 4π. Therefore the first transition curve is obtained by setting $n = 0$, which gives $\alpha_0 = 0$ and $\psi_0 = 1$ by (A.2a). For $k = 1$, (A.3a) gives

$$\ddot{\psi}_1(t) + \alpha_1 + \cos t = 0,$$

which yields $\alpha_1 = 0$ and $\psi_1(t) = \cos t$. Then, one can easily prove by induction that $\alpha_k = 0$ and $\psi_k(t) = 0$ for all $k \geq 2$. Indeed, (A.3b) becomes

$$\ddot{\psi}_2(t) + \alpha_2 - \cos^2 t + \cos^2 t = \ddot{\psi}_2(t) + \alpha_2 = 0,$$

while for $k > 2$, by using the inductive hypothesis, one finds

$$\ddot{\psi}_k(t) + \alpha_k + \cos t \left((-\cos t)^{k-1} + (-\cos t)^{k-2} \psi_1(t) \right) = \ddot{\psi}_k(t) + \alpha_k = 0.$$

This shows that $\alpha(\varepsilon) = 0$ and $\psi(t, \varepsilon) = 1 + \varepsilon \cos t$. The solution has been found formally by assuming ε to be small, but, as the series reduces to a polynomial, in fact is defined and solves the equation for all values $|\varepsilon| < 1$. Therefore the first transition curve is defined by $\alpha(\varepsilon) = 0$ — and as a by-product of the construction, the corresponding periodic solution is $\psi(t, \varepsilon) = 1 + \varepsilon \cos t$.

Appendix B. Equations of motion in action-angle variables

We begin by describing the dynamics of the simple pendulum in action-angle variables (I, φ); see [55, 34] for the general theory and [26, 65] for the application to the pendulum.

The equations of motion for the simple pendulum, to which both (2) and (3) reduce for $\delta = 0$ and $\varepsilon = 0$, respectively, is $\ddot{\theta} + \alpha \sin\theta = 0$. Let $\mathbf{K}(k)$ and $\mathbf{E}(k)$ be the complete elliptic integrals of the first and second kind with elliptic modulus k [25, 29, 44, 64] — see also [26, 65] for details on the forthcoming discussion. Let $k_1 \in (0,1)$ be such that $k_1^2 = (E+\alpha)/2\alpha$, with E being the energy of the pendulum (fixed by the initial condition), and set $k_2 = 1/k_1$. The action variable for the pendulum is

$$I = \frac{8}{\pi}\sqrt{\alpha}\Big[(k_1^2 - 1)\mathbf{K}(k_1) + \mathbf{E}(k_1)\Big], \qquad I = \frac{4}{k_2 \pi}\sqrt{\alpha}\,\mathbf{E}(k_2), \tag{B.1}$$

for librations inside the separatrix and for rotations outside, respectively. Then, by setting $(q,p) = (\theta, \dot{\theta})$, the transformation to action-angle variables $(p,q) \mapsto (I, \varphi)$ is given by

$$p = 2k_1\sqrt{\alpha}\,\mathrm{cn}\left(\frac{2\mathbf{K}(k_1)}{\pi}\varphi, k_1\right), \qquad q = 2\arcsin\left[k_1\,\mathrm{sn}\left(\frac{2\mathbf{K}(k_1)}{\pi}\varphi, k_1\right)\right] \tag{B.2}$$

for the dynamics inside the separatrix, and by

$$p = \frac{2}{k_2}\sqrt{\alpha}\,\mathrm{dn}\left(\frac{\mathbf{K}(k_2)}{\pi}\varphi, k_2\right), \qquad q = 2\arcsin\left[\mathrm{sn}\left(\frac{\mathbf{K}(k_2)}{\pi}\varphi, k_2\right)\right] \tag{B.3}$$

for the dynamics outside the separatrix, where k_1 and k_2 are expressed in terms of I by inverting the relations (B.1). Here $\mathrm{cn}\,(u,k)$, $\mathrm{sn}(u,k)$ and $\mathrm{dn}(u,k)$ are the Jacobi elliptic functions with elliptic modulus k [29, 44, 64]. In terms of the action-angle variables, the motion is a uniform rotation, with I being fixed and

$$\varphi(t) = \frac{\pi}{2\mathbf{K}(k_1)}\sqrt{\alpha}\,(t - t_0), \qquad \varphi(t) = \frac{\pi}{\mathbf{K}(k_2)}\sqrt{\alpha}\,\frac{t-t_0}{k_2}, \tag{B.4}$$

for librations and rotations, respectively, with the parameter t_0 depending on the initial condition. Explicit calculations are given in [65, Appendix 2], which we refer to for further details. From (B.4) it can be seen that the solutions are functions of $(t - t_0)$, so that the phase of a solution depends on the initial conditions. Without loss of generality we can fix the phase of the solution to zero by writing $f(t)$ in equation (8) as $f(t-t_0)$, and similarly for $h(t)$ and $g(t)$ in equation (12). This moves the freedom of choice in the initial condition to the phase of the forcing.

In order to write the equations of motion for the system (3) in terms of the action-angle variables (I, φ), we shall use that

$$\begin{pmatrix} \partial\varphi/\partial q & \partial\varphi/\partial p \\ \partial I/\partial q & \partial I/\partial p \end{pmatrix} = \begin{pmatrix} \partial p/\partial I & -\partial q/\partial I \\ -\partial p/\partial\varphi & \partial q/\partial\varphi \end{pmatrix}, \tag{B.5}$$

since the transformation to action-angle variables is canonical.

Appendix B.1. Librations

First we consider the librations and write the equations of motions for the perturbed system (3) in the absence of dissipation. Using (B.5), the time derivative of the action is

$$\begin{aligned}\dot{I} &= \frac{\partial I}{\partial q}\dot{q} + \frac{\partial I}{\partial p}\dot{p} = -\frac{\partial p}{\partial\varphi}\dot{q} + \frac{\partial q}{\partial\varphi}\dot{p} \\ &= \frac{4\sqrt{\alpha}k_1\mathbf{K}(k_1)\,\mathrm{sn}(\cdot)\,\mathrm{dn}(\cdot)}{\pi}p - \frac{4k_1\mathbf{K}(k_1)\,\mathrm{cn}(\cdot)}{\pi}\left[-\frac{2\varepsilon\sin(t-t_0)}{1+\varepsilon\cos(t-t_0)}p + \frac{\alpha}{1+\varepsilon\cos(t-t_0)}\sin q\right],\end{aligned}$$

where we are shortening $(\cdot) = (2\mathbf{K}(k_1)\varphi/\pi, k_1)$. Using that $\sin(2\arcsin(kx)) = 2kx\sqrt{1-k^2x^2}$, we may rewrite the above as

$$\dot{I} = \frac{8k_1^2\alpha\mathbf{K}(k_1)\,\mathrm{sn}(\cdot)\,\mathrm{cn}(\cdot)\,\mathrm{dn}(\cdot)}{\pi}\left(1 - \frac{1}{1+\varepsilon\cos(t-t_0)}\right) + \frac{16k_1^2\sqrt{\alpha}\mathbf{K}(k_1)\varepsilon\sin(t-t_0)\,\mathrm{cn}^2(\cdot)}{\pi(1+\varepsilon\cos(t-t_0))},$$

where, for ε small, we can expand

$$\frac{1}{1+\varepsilon\cos(t-t_0)} = \sum_{n=0}^{\infty}(-\varepsilon\cos(t-t_0))^n.$$

In the calculation of $\dot{\varphi}$ it is required to differentiate p and q with respect to the action I. The dependence of p and q on the action I is not explicitly obvious from (B.2), however the dependence on the elliptic modulus $k = k_1$ is clear and we use the relation [26, 65]

$$\frac{\partial}{\partial I} = \frac{\partial k}{\partial I}\left(\frac{\partial}{\partial k} + \frac{\partial u}{\partial k}\frac{\partial}{\partial u}\right).$$

where u is the first argument of the functions, i.e. $\mathrm{sn}(u,k)$, etc. Doing so we find

$$\begin{aligned}\dot{\varphi} = \frac{\partial \varphi}{\partial q}\dot{q} - \frac{\partial \varphi}{\partial p}\dot{p} = \frac{\partial p}{\partial I}\dot{q} - \frac{\partial q}{\partial I}\dot{p} = \frac{\pi\sqrt{\alpha}}{2\mathbf{K}(k_1)}\Bigg\{1 + \Bigg[\mathrm{sn}^2(\cdot) + \frac{2\mathbf{E}(k_1)\varphi\,\mathrm{sn}(\cdot)\,\mathrm{cn}(\cdot)\,\mathrm{dn}(\cdot)}{\pi(1-k_1^2)} \\ + \frac{k_1^2\,\mathrm{sn}^2(\cdot)\,\mathrm{cn}^2(\cdot)}{1-k_1^2} - \frac{\mathbf{E}(\cdot)\,\mathrm{sn}(\cdot)\,\mathrm{cn}(\cdot)\,\mathrm{dn}(\cdot)}{1-k_1^2}\Bigg]\sum_{n=1}^{\infty}(-\varepsilon\cos(t-t_0))^n\Bigg\} \\ - \frac{\pi\varepsilon\sin(t-t_0)\,\mathrm{cn}(\cdot)}{\mathbf{K}(k_1)}\left[\frac{\mathrm{sn}(\cdot)}{\mathrm{dn}(\cdot)} + \frac{2\mathbf{E}(k_1)\varphi\,\mathrm{cn}(\cdot)}{\pi(1-k_1^2)} + \frac{k_1^2\,\mathrm{sn}(\cdot)\,\mathrm{cn}^2(\cdot)}{(1-k_1^2)\,\mathrm{dn}(\cdot)} - \frac{\mathbf{E}(\cdot)\,\mathrm{cn}(\cdot)}{1-k_1^2}\right]\sum_{n=0}^{\infty}(-\varepsilon\cos(t-t_0))^n,\end{aligned}$$

where $\mathbf{E}(u,k)$ is the incomplete elliptic integral of the second kind [44]. In order to take into account the dissipative term $\zeta\dot{q}$ we note that

$$\dot{q} = \frac{\partial q}{\partial I}\dot{I} + \frac{\partial q}{\partial \varphi}\dot{\varphi} = 2k_1\sqrt{\alpha}\,\mathrm{cn}(\cdot),$$

and, using the relation $\mathbf{E}(u,k) = \mathbf{E}(k)u/\mathbf{K}(k) + \mathbf{Z}(u,k)$, where $\mathbf{Z}(u,k)$ is the Jacobi zeta function [26, 44], we arrive at the equations of motion

$$\begin{aligned}\dot{I} &= -\frac{8k_1^2\alpha\mathbf{K}(k_1)\,\mathrm{sn}(\cdot)\,\mathrm{cn}(\cdot)\,\mathrm{dn}(\cdot)}{\pi}\sum_{n=1}^{\infty}(-\varepsilon\cos(t-t_0))^n \\ &\quad + \frac{16k_1^2\sqrt{\alpha}\mathbf{K}(k_1)\varepsilon\sin(t-t_0)\,\mathrm{cn}^2(\cdot)}{\pi}\sum_{n=0}^{\infty}(-\varepsilon\cos(t-t_0))^n - \frac{8\zeta k_1^2\sqrt{\alpha}\mathbf{K}(k_1)\,\mathrm{cn}^2(\cdot)}{\pi}, \\ \dot{\varphi} &= \frac{\pi\sqrt{\alpha}}{2\mathbf{K}(k_1)}\left\{1 + \left[\mathrm{sn}^2(\cdot) + \frac{k_1^2\,\mathrm{sn}^2(\cdot)\,\mathrm{cn}^2(\cdot)}{1-k_1^2} - \frac{\mathbf{Z}(\cdot)\,\mathrm{sn}(\cdot)\,\mathrm{cn}(\cdot)\,\mathrm{dn}(\cdot)}{1-k_1^2}\right]\sum_{n=1}^{\infty}(-\varepsilon\cos(t-t_0))^n\right\} \\ &\quad - \frac{\pi\varepsilon\sin(t-t_0)\,\mathrm{cn}(\cdot)}{\mathbf{K}(k_1)}\left[\frac{\mathrm{sn}(\cdot)}{\mathrm{dn}(\cdot)} + \frac{k_1^2\,\mathrm{sn}(\cdot)\,\mathrm{cn}^2(\cdot)}{(1-k_1^2)\,\mathrm{dn}(\cdot)} - \frac{\mathbf{Z}(\cdot)\,\mathrm{cn}(\cdot)}{1-k_1^2}\right]\sum_{n=0}^{\infty}(-\varepsilon\cos(t-t_0))^n \\ &\quad + \frac{\zeta\sqrt{\alpha}\pi\,\mathrm{cn}(\cdot)}{2\mathbf{K}(k_1)}\left[\mathrm{cn}(\cdot) - \frac{k_1^2\,\mathrm{sn}^2(\cdot)\,\mathrm{cn}(\cdot)}{1-k_1^2} + \frac{\mathbf{Z}(\cdot)\,\mathrm{sn}(\cdot)\,\mathrm{dn}(\cdot)}{1-k_1^2}\right].\end{aligned} \tag{B.6}$$

Then, in (B.6), we expand formally

$$\zeta = \sum_{k=1}^{\infty} \varepsilon^k C_k, \qquad I(t) = \sum_{k=0}^{\infty} \varepsilon^k I^{(k)}(t), \qquad \varphi(t) = \sum_{k=0}^{\infty} \varepsilon^k \varphi^{(k)}(t), \tag{B.7}$$

where

$$I^{(0)}(t) = I^{(0)} := \frac{8}{\pi}\sqrt{\alpha}\Big[(k_1^2-1)\mathbf{K}(k_1) + \mathbf{E}(k_1)\Big], \qquad \varphi^{(0)} = \frac{\pi}{2\mathbf{K}(k_1)}\sqrt{\alpha}\, t, \tag{B.8}$$

according to (B.1) and (B.4), and fix recursively the constants C_k in such a way that the functions $I^{(k)}(t)$ and $\varphi^{(k)}(t)$ are periodic with period $T := 2\pi q = 4\mathbf{K}(k_1)p/\sqrt{\alpha}$, with $p/q \in \mathbb{Q}$, for all $k \geq 1$. By inserting (B.7) into (B.6), we obtain

$$\begin{aligned} \varepsilon \dot{I}^{(1)}(t) + \varepsilon^2 \dot{I}^{(2)}(t) + \ldots &= \varepsilon F_2^{(1)}(t) + \varepsilon^2 F_2^{(2)}(t) + \ldots, \\ \dot{\varphi}^{(0)}(t) + \varepsilon \dot{\varphi}^{(1)}(t) + \varepsilon^2 \dot{\varphi}^{(2)}(t) + \ldots &= \varepsilon F_1^{(1)}(t) + \varepsilon^2 F_1^{2)}(t) + \ldots, \end{aligned}$$

where both functions $F_2^{(k)}(t)$ and $F_1^{(k)}(t)$ depend on the functions $I^{(h)}(t)$ and $\varphi^{(h)}(t)$, with $h < k$ only, so that the equations can be solved iteratively — we refer [65, Section 2.1] for details. To any order the condition for the solution to be periodic turns out to be

$$\langle F_2^{(k)} \rangle := \frac{1}{T}\int_0^T \mathrm{d}t\, F_2^{(k)}(t) = 0, \tag{B.9}$$

which fixes the value of the constant C_k. For instance, to first order one finds, from (B.6) and (B.8),

$$F_2^{(1)}(t) = \frac{8k_1^2 \mathbf{K}(k_1)\sqrt{\alpha}}{\pi}\Big(\sqrt{\alpha}\,\mathrm{sn}(\sqrt{\alpha}t)\,\mathrm{cn}(\sqrt{\alpha}t)\,\mathrm{dn}(\sqrt{\alpha}t)\cos(t-t_0) + (2\sin(t-t_0) - C_1)\,\mathrm{cn}^2(\sqrt{\alpha}t)\Big),$$

so that the condition (B.9) for $k = 1$ yields

$$C_1 \int_0^T \mathrm{d}t\ \mathrm{cn}^2(\sqrt{\alpha}t) = \int_0^T \mathrm{d}t\Big(\sqrt{\alpha}\,\mathrm{sn}(\sqrt{\alpha}t)\ \mathrm{cn}(\sqrt{\alpha}t)\ \mathrm{dn}(\sqrt{\alpha}t)\ \cos(t-t_0) + 2\sin(t-t_0)\ \mathrm{cn}^2(\sqrt{\alpha}t)\Big).$$

For the integrals on the right hand side not to vanish, one needs $p = 1$ and q even (see again [65] for more details). By computing explicitly the integrals, for $\alpha = 0.5$ and k_1 such that $2\mathbf{K}(k_1) = \pi\sqrt{\alpha}q$, with q even, and taking the maximum over t_0, one finds the values listed in Table 3.

Appendix B.2. Rotations

For the rotations of the perturbed system without dissipation, the equations of motion are

$$\begin{aligned} \dot{I} &= -\frac{\partial p}{\partial \varphi}\dot{q} + \frac{\partial q}{\partial \varphi}\dot{p} = -\frac{4\alpha \mathbf{K}(k_2)\,\mathrm{sn}(\cdot)\,\mathrm{cn}(\cdot)\,\mathrm{dn}(\cdot)}{\pi}\sum_{n=1}^{\infty}(-\varepsilon\cos(t-t_0))^n \\ &\quad + \frac{8\mathbf{K}(k_2)\varepsilon\sin(t-t_0)\sqrt{\alpha}\,\mathrm{dn}^2(\cdot)}{\pi k_2}\sum_{n=0}^{\infty}(-\varepsilon\cos(t-t_0))^n, \\ \dot{\varphi} &= \frac{\partial p}{\partial I}\dot{q} - \frac{\partial q}{\partial I}\dot{p} = \frac{\pi k_2 \sqrt{\alpha}}{\mathbf{K}(k_2)}\left[\frac{1}{k_2^2} - \left(\frac{\varphi \mathbf{E}(k)\,\mathrm{sn}(\cdot)\,\mathrm{cn}(\cdot)\,\mathrm{dn}(\cdot)}{\pi(1-k_2^2)}\right.\right. \\ &\qquad \left.\left. + \frac{k_2^2\,\mathrm{sn}^2(\cdot)\,\mathrm{cn}^2(\cdot)}{1-k_2^2} - \frac{\mathbf{E}(\cdot)\,\mathrm{sn}(\cdot)\,\mathrm{cn}(\cdot)\,\mathrm{dn}(\cdot)}{(1-k_2^2)}\right)\sum_{n=1}^{\infty}(-\varepsilon\cos(t-t_0))^n\right] \\ &\quad + \frac{2\varepsilon\pi\sin(t-t_0)\,\mathrm{dn}(\cdot)}{\mathbf{K}(k_2)}\left[\frac{\varphi \mathbf{E}(k_2)\,\mathrm{dn}(\cdot)}{\pi k_2(1-k_2^2)} + \frac{k_2\,\mathrm{sn}(\cdot)\,\mathrm{cn}(\cdot)}{1-k_2^2} - \frac{\mathbf{E}(\cdot)\,\mathrm{dn}(\cdot)}{k_2(1-k_2^2)}\right]\sum_{n=0}^{\infty}(-\varepsilon\cos(t-t_0))^n, \end{aligned}$$

where $(\cdot) = (\mathbf{K}(k_2)\varphi/\pi, k_2)$. Note that the following equality, which may be derived using the identities for the Jacobi elliptic functions [44], was used in finding the expression for $\dot{\varphi}$

$$\begin{aligned}\frac{\mathrm{dn}^2}{k^2} - \frac{k^2\,\mathrm{sn}^2\,\mathrm{cn}^2}{1-k^2} + \frac{\mathrm{sn}^2\,\mathrm{dn}^2}{1-k^2} &= \frac{\mathrm{dn}^2}{k^2} - \frac{k^2\,\mathrm{sn}^2(1-\mathrm{sn}^2)}{1-k^2} + \frac{\mathrm{sn}^2\,\mathrm{dn}^2}{1-k^2} \\ &= \frac{\mathrm{dn}^2}{k^2} + \frac{\mathrm{sn}^2}{1-k^2}\Big[\mathrm{dn}^2 - k^2 + k^2\,\mathrm{sn}^2\Big] = \frac{\mathrm{dn}^2}{k^2} + \frac{\mathrm{sn}^2}{1-k^2}\Big[1-k^2\Big] = \frac{1}{k^2}\Big[\mathrm{dn}^2 + k^2\,\mathrm{sn}^2\Big] = \frac{1}{k^2}.\end{aligned}$$

The term $\zeta\dot{q}$ may be calculated in the same way as for the librations and we find that, with the inclusion of friction, the action-angle variables satisfy

$$\begin{aligned}\dot{I} &= -\frac{4\alpha\mathbf{K}(k_2)\,\mathrm{sn}(\cdot)\,\mathrm{cn}(\cdot)\,\mathrm{dn}(\cdot)}{\pi}\sum_{n=1}^{\infty}(-\varepsilon\cos(t-t_0))^n \\ &\quad + \frac{8\mathbf{K}(k_2)\varepsilon\sin(t-t_0)\sqrt{\alpha}\,\mathrm{dn}^2(\cdot)}{\pi k_2}\sum_{n=0}^{\infty}(-\varepsilon\cos(t-t_0))^n - \frac{4\zeta\sqrt{\alpha}\mathbf{K}(k_2)\,\mathrm{dn}^2(\cdot)}{k_2\pi}, \\ \dot{\varphi} &= \frac{\pi k_2\sqrt{\alpha}}{\mathbf{K}(k_2)}\left[\frac{1}{k_2^2} - \left(\frac{k_2^2\,\mathrm{sn}^2(\cdot)\,\mathrm{cn}^2(\cdot)}{1-k_2^2} - \frac{\mathbf{Z}(\cdot)\,\mathrm{sn}(\cdot)\,\mathrm{cn}(\cdot)\,\mathrm{dn}(\cdot)}{(1-k_2^2)}\right)\sum_{n=1}^{\infty}(-\varepsilon\cos(t-t_0))^n\right] \\ &\quad + \frac{2\varepsilon\pi\sin(t-t_0)\,\mathrm{dn}(\cdot)}{\mathbf{K}(k_2)}\left[\frac{k_2\,\mathrm{sn}(\cdot)\,\mathrm{cn}(\cdot)}{1-k_2^2} - \frac{\mathbf{Z}(\cdot)\,\mathrm{dn}(\cdot)}{k_2(1-k_2^2)}\right]\sum_{n=0}^{\infty}(-\varepsilon\cos(t-t_0))^n \\ &\quad + \frac{\zeta\sqrt{\alpha}\pi k_2\,\mathrm{dn}(\cdot)}{\mathbf{K}(k_2)}\left[\frac{\mathrm{dn}(\cdot)}{k_2^2} + \frac{\mathrm{sn}^2(\cdot)\,\mathrm{dn}(\cdot)}{1-k_2^2} - \frac{\mathbf{Z}(\cdot)\,\mathrm{sn}(\cdot)\,\mathrm{cn}(\cdot)}{1-k_2^2}\right].\end{aligned} \tag{B.10}$$

To determine the constants C_k one proceeds as in the case of librations, the only difference being that now

$$F_2^{(1)}(t) = \frac{4\mathbf{K}(k_2)\sqrt{\alpha}}{\pi k_2}\Big(\sqrt{\alpha}k_2\cos(t-t_0)\,\mathrm{sn}(\sqrt{\alpha}t)\,\mathrm{cn}(\sqrt{\alpha}t)\,\mathrm{dn}(\sqrt{\alpha}t) + (2\sin(t-t_0)-C_1)\,\mathrm{dn}^2(\sqrt{\alpha}t)\Big)$$

which requires once more $p = 1$ and q even; then, by fixing q, choosing k_2 so that $2k_2\mathbf{K}(k_2) = \pi\sqrt{\alpha}q$ and taking the maximu over t_0, one finds the values of C_1 given in Table 4.

[1] D. Acheson, *A pendulum theorem*, Proc. Roy. Soc. London Ser. A **443** (1993), no. 1917, 239-245.

[2] D. Acheson, T. Mullin, *Upside-down pendulums*, Nature **366** (1993), 215-216.

[3] D. Acheson, T. Mullin, *Ropy magic*, New Scientist **157** (1998), 32-33.

[4] L.D. Akulenko, S.V. Nesterov, *The stability of the equilibrium of a pendulum of variable length*, Prikl. Mat. Mekh. **73** (2009), no. 6, 893-901; translation in J. Appl. Math. Mech. **73** (2009), no. 6, 642-647. *Erratum*, J. Appl. Math. Mech. **74** (2010), no. 2, 253.

[5] F.M. Arscott, *Periodic differential equations. An introduction to Mathieu, Lamé, and allied functions*, Pergamon Press, New York, 1964.

[6] B.S. Bardin, A.P. Markeev, *On the stability of equilibrium of a pendulum with vertical oscillations of its suspension point*, Prikl. Mat. Mekh. **59** (1995), no. 6, 922-929; translation in J. Appl. Math. Mech. **59** (1995), no. 6, 879-886 (1996).

[7] M.V. Bartuccelli, A. Berretti, J.H.B. Deane, G. Gentile, S.A. Gourley, *Selection rules for periodic orbits and scaling laws for a driven damped quartic oscillator*, Nonlinear Anal. Real World Appl. **9** (2008), no. 5, 1966-1988.

[8] M.V. Bartuccelli, P.L. Christiansen, V. Muto, M.P. Soerensen, N.F. Pedersen, *Chaotic behaviour of a pendulum with variable length*, Nuovo Cimento B **100** (1988), no. 2, 229-249.

[9] M.V. Bartuccelli, J.H.B. Deane, G. Gentile, *Globally and locally attractive solutions for quasi-periodically forced systems*, J. Math. Anal. Appl. **328** (2007), no. 1, 699-714.

[10] M.V. Bartuccelli, J.H.B. Deane, G. Gentile, *Attractiveness of periodic orbits in parametrically forced systems with time-increasing friction*, J. Math. Physics **53** (2012), no. 10, 102703, 27 pp.

[11] M.V. Bartuccelli, J.H.B. Deane, G. Gentile, S.A. Gourley, *Global attraction to the origin in a parametrically-driven nonlinear oscillator*, Appl. Math. Comput. **153** (2004), no. 1, 1-11.

[12] M.V. Bartuccelli, G. Gentile, K.V. Georgiou, *On the dynamics of a vertically driven damped planar pendulum*, R. Soc. Lond. Proc. Ser. A Math. Phys. Eng. Sci. **457** (2001), no. 2016, 3007-3022 .

[13] M.V. Bartuccelli, G. Gentile, K.V. Gergiou, *On the stability of the upside-down pendulum with damping*, R. Soc. Lond. Proc. Ser. A Math. Phys. Eng. Sci. **458** (2002), no. 2018, 255-269 .

[14] M.V. Bartuccelli, G. Gentile, K.V. Georgiou, *KAM theory, Lindstedt series and the stability of the upside-down pendulum*, Discrete Contin. Dyn. Syst. Ser. A. **9** (2003), no. 2, 413-426.

[15] M.V. Bartuccelli, G. Gentile, J.A. Wright, *On a class of Hill's equations having explicit solutions*, Appl. Math. Lett. **26** (2013), no. 10, 1026-1030.

[16] A.O. Belyakov, A.P. Seyranian, *A remark on the paper by L. D. Akulenko and S. V. Nesterov "Stability of the equilibrium of a pendulum of variable length"*, Prikl. Mat. Mekh. **75** (2011), no. 4, 701; translation in J. Appl. Math. Mech. **75** (2011), no. 4, 491.

[17] A.O. Belyakov, A.P. Seyranian, *Dynamics of a pendulum of varying length and similar problems*, Chapter 4 in *Nonlinearity, Bifurcation and Chaos - Theory and Applications*, INTECH, Rijeka, 2012.

[18] A.O. Belyakov, A.P. Seyranian, *Homoclinic, subharmonic, and superharmonic bifurcations for a pendulum with periodically varying length*, Nonlinear Dynam. **77** (2014), no. 4, 1617-1627.

[19] A. Belyakov, A.P. Seyranian, A. Luongo, *Dynamics of the pendulum with periodically varying length*, Phys. D **238** (2009), no. 16, 1589-1597.

[20] S.R. Bishop, M.J. Clifford, *Non rotating periodic orbits in the parametrically excited pendulum*, European J. Mech. A Solids **13** (1994), no. 4, 581-587.

[21] S.R. Bishop, M.J. Clifford, *The use of manifold tangencies to predict orbits, bifurcations and estimate escape in driven systems*, Chaos Solitons Fractals **7** (1996), no 10, 1537-1553.

[22] S.R. Bishop, D.L. Xu, M.J. Clifford, *Flexible control of the parametrically excited pendulum*, R. Soc. Lond. Proc. Ser. A Math. Phys. Eng. Sci. **452** (1996), no. 1951, 1789-1806.

[23] N.N. Bogolyubov, Yu.A. Mitropolsky, *Asymptotic methods in the theory of nonlinear oscillations*, Gordon and Breach, New York, 1961.

[24] A. Boscaggin, F. Zanolin, *Subharmonic solutions for nonlinear second order equations in presence of lower and upper solutions*, Discrete Contin. Dyn. Syst. **33** (2013), no. 1, 89-110.

[25] F. Bowman, *Introduction to elliptic functions with applications*, English Universities Press, London, 1953.

[26] A.J. Brizard, *Jacobi zeta function and action-angle coordinates for the pendulum*, Commun. Nonlinear Sci. Numer. Simul. **18** (2013), no. 3, 511-518.

[27] P.J. Bryant, J.W. Miles, *On a periodically forced, weakly damped pendulum. Part 3: vertical forcing*, J. Austral. Math. Soc. Ser. B, **32** (1990), 42-60.

[28] L. Burra, *Chaotic dynamics in nonlinear theory*, Springer, New Delhi, 2014.

[29] P.F. Byrd, M.D. Friedman, *Handbook of elliptic integrals for engineers and scientists*, Second edition - revised, Springer, New York-Heidelberg, 1971.

[30] D. Capecchi, S.R. Bishop, *Periodic oscillations and attracting basins for a parametrically excited pendulum*, Dynam. Stability Systems, **9** (1994), no. 2, 123-143.

[31] M.J. Clifford, S.R. Bishop, *Inverted oscillations of a driven pendulum*, R. Soc. Lond. Proc. Ser. A Math. Phys. Eng. Sci. **454** (1998), no. 1979, 2811-2817.

[32] M.J. Clifford, S.R. Bishop, *Rotating periodic orbits of the parametrically excited pendulum*, Phys. Lett. A **201** (1995), 191-196.

[33] M.J. Clifford, S.R. Bishop, *Locating oscillatory orbits of the parametrically excited pendulum*, J. Austral. Math. Soc. Ser. B **37** (1996), no. 3, 309-319.

[34] A. Fasano, S. Marmi, *Analytical Mechanics*, Oxford University Press, Oxford, 2006.

[35] U. Feudel, C. Grebogi, *Why are chaotic attractors rare in multistable systems*, Phys. Rev. E **91** (2003), 134102, 4 pp.

[36] M. Furi, M. Martelli, M. O'Neill, C. Staples, *Chaotic orbits of a pendulum with varying length*, Electron. J. Differential Equations **2004** (2004), no. 36, 14 pp.

[37] W. Garira, S.R. Bishop, *Oscillatory orbits of the parametrically excited pendulum*, Internat. J. Bifur. Chaos Appl. Sci. Engrg. **13** (2003), no. 10, 2949-2958.

[38] J. Guckenheimer, Ph. Holmes, *Nonlinear oscillations, dynamical systems, and bifurcations of vector fields*, Revised and corrected reprint of the 1983 original, Applied Mathematical Sciences Vol. 42, Springer, New York, 1990.

[39] B. Horton, J. Sieber, J.M.T. Thompson, M. Wiercigroch, *Dynamics of the nearly parametric pendulum*, Internat. J. Non-Linear Mech. **46** (2011), no. 2, 436-442.

[40] D.W. Jordan, P. Smith, *Nonlinear ordinary differential equations. An introduction for scientists and engineers*, Fourth edition, Oxford University Press, Oxford, 2007.

[41] P. L. Kapitsa, *Dynamic stability of a pendulum with a vibrating point of suspension*, Zh. Eksp. Teoret. Fiz. **21** (1951), 588-598; translated in *Collected papers by P. L. Kapitsa*, ed. D. ter Haar, vol. 2, pp. 714726, Pergamon, London, 1965.

[42] S.Y. Kim, B. Hu, *Bifurcations amd Transitions to Chaos in an Inverted Pendulum*, Phys. Rev. E. **58** (1998), no. 3, 3028-3035.

[43] B.P. Koch, R.W. Leven *Subharmonic and homoclinic bifurcations in a parametrically forced pendulum*, Phys. D **16** (1985), 1-13.

[44] D.F. Lawden, *Elliptic functions and applications*, Springer, New York, 1989.

[45] S. Lenci, E. Pavlovskaia, G. Rega, M. Wiercigroch, *Rotating solutions and stability of parametric pendulum by perturbation method*, J. Sound Vibration **310** (2008), 243-259.

[46] W. Magnus, S. Winkler, *Hill's Equation*, Corrected reprint of the 1966 edition, Dover, New York, 2004.

[47] F.J. McCormick, J.A. Witz, *An investigation into the parametric excitation of suspended loads during crane vessel operations*, J. Underwater Technology **19**, 30-39 .

[48] R. McLachlan, M. Perlmutter, *Conformal Hamiltonian systems*, J. Geom. Phys. **39** (2001), no. 4, 276-300.

[49] B.E. Moore, *A modified equations approach for multi-symplectic integration methods*, Thesis, University of Surrey, 2003.

[50] T. Mullin, A. Champneys, W.B. Fraser, J. Galan, D. Acheson, *The "Indian wire trick" via parametric excitation: a comparison between theory and experiment*, R. Soc. Lond. Proc. Ser. A Math. Phys. Eng. Sci. **459** (2003), no. 2031, 539-546.

[51] R.H. Myers, S.L. Myers, R.E. Walpole, *Probability and statistics for engineers and scientists*, Sixth edition, Prentice Hall, London, 1998.

[52] D. Núñez, R. Ortega, *Parabolic fixed points and stability criteria for nonlinear Hill's equation*, Z. Angew. Math. Phys. **51** (2000), no. 6, 890-911.

[53] R. Ortega, *The stability of the equilibrium of a nonlinear Hill's equation*, Siam J. Math. Anal. **25** (1994), no. 5, 1393-1401.

[54] Y.G. Panovko, I.I. Gabanova, *Stability and oscillation of elastic systems: Modern concepts, paradoxes and errors*, Second edition, Nasa technical translations, 1973.

[55] I. Percival, D. Richards, *Introduction to dynamics*, First edition - reprint, Cambridge University Press, Cambridge, 1994.

[56] V.A. Pliss, *Nonlocal problems of the theory of oscillations*, Academic Press, New York-London, 1966.

[57] M.A. Pinsky, A.A. Zevin, *Oscillations of a pendulum with a periodically varying length and a model of swing*, Internat. J. Non-Linear Mech. **34** (1999), no. 1,105-109.

[58] R.C.T. Rainey, *The dynamics of tethered platforms*, Trans. Royal Inst. Naval Architects **120** (1978), 59-80.

[59] A.P. Seyranian, *Swing problem*, Dokl. Phys. **49** (2004), no.1, 64-68.

[60] A.C. Skeldon, *Dynamics of a parametrically excited double pendulum*, Phys. D **75** (1994), no. 4, 541-558.

[61] A. Sofroniou, S.R. Bishop, *Breaking the symmetry of the parametrically excited pendulum*, Chaos Solitons Fractals **28** (2006), no. 3, 673-681.

[62] A. Stephenson, *On a new type of dynamical stability*, Mem. Proc. Manch. Lit. Phil. Soc. **52** (1908), 1-10.

[63] D.J. Sudor, S.R. Bishop, *Inverted dynamics of a tilted parametric pendulum*, European J. Mech. A Solids **18** (1999), no. 3, 517-526.

[64] E. T. Whittaker, G.N. Watson, *A course of modern analysis*, Fourth edition - reprint, Cambridge University Press, Cambridge, 1947.

[65] J.A. Wright, M. Bartuccelli, G. Gentile, *The effects of time-dependent dissipation on the basins of attraction for the pendulum with oscillating support*, Nonlinear Dynam. **77** (2014), no. 4, 1377-1409.

[66] J.A. Wright, J.H.B. Deane, M. Bartuccelli, G. Gentile, *Basins of attraction in forced systems with time-varying dissipation*, Commun. Nonlinear Sci. Numer. Simul. **29** (2015), 72-87.

[67] X. Xu, M. Wiercigroch, M.P. Cartmell, *Rotating orbits of a paramtrically-excited pendulum*, Chaos Solitons Fractals **23** (2005), no.5, 1537-1548.